Journal of Environmental Chemical Engineering 12 (2024) 114106

Contents lists available at ScienceDirect

Journal of Environmental Chemical Engineering

journal homepage: www.elsevier.com/locate/jece

Membrane materials for biogas purification and upgrading: Fundamentals, recent advances and challenges

María del Rosario Rodero [a,b,*], Raúl Muñoz [a,b], Armando González-Sánchez [c], Héctor A. Ruiz [d], Guillermo Quijano [e,**]

[a] Institute of Sustainable Processes, University of Valladolid, Valladolid 47011, Spain
[b] Department of Chemical Engineering and Environmental Technology, University of Valladolid, Dr. Mergelina s/n., Valladolid 47011, Spain
[c] Instituto de Ingeniería, Universidad Nacional Autónoma de México, Circuito Escolar, Ciudad Universitaria, Mexico City 04510, Mexico
[d] Biorefinery Group, Food Research Department, School of Chemistry, Autonomous University of Coahuila, Saltillo, Coahuila 25280, Mexico
[e] NextGenBiotech, Department of Process Engineering. Horticultura, 51, Venustiano Carranza, Ciudad de Mexico 15340, Mexico

ARTICLE INFO

Keywords:
Biogas separation
Carbon dioxide removal
Biofuels
Biomethane
Membrane performance

ABSTRACT

Biogas from the anaerobic digestion of organic waste stands as a renewable energy source with a large potential to reduce the global dependence on fossil fuels. Biogas applications as a vehicle fuel or natural gas substitute requires the separation of the main biogas components, namely methane and carbon dioxide. Such biogas separation is also necessary for valorizing carbon dioxide, which is a valuable molecule in food and beverage industries, chemical synthesis and greenhouses, among other industrial activities. While most biological technologies focused on biogas separation are still in the development phase, the use of membranes for this purpose has increased exponentially in the last decade due to its efficiency, compact design, economic feasibility, and easy scalability. This article provides a comprehensive overview of the current state of membrane technology, focusing on both fundamental principles and the latest advancements in membrane systems for biogas purification and upgrading. 6FDA-based polyimides and polymers of intrinsic microporosity offer promising prospects for advancing membrane technologies used in biogas upgrading. The incorporation of fillers, such as zeolites and metal-organic frameworks, into a polymer matrix to create mixed matrix membranes (MMMs) significantly enhances the overall performance (CO_2 permeabilities up to 18,000 Barrer and CO_2/CH_4 selectivity values up to 85) and functionality of the membrane. However, the key challenges for MMMs remain in fabricating defect-free membranes with high CO_2/CH_4 selectivity and ensuring long-term stability over several months.

1. Introduction

Nowadays, approximately 80 % of the global energy demand is primarily supplied by fossil fuels [1]. Extraction, refining and combustion of fossil fuels are activities with negative consequences to the environment, including direct emissions of greenhouse gases to the atmosphere as well as impacts on aquatic and terrestrial ecosystems [2,3]. In the past two decades, many initiatives have been proposed for switching energy production towards alternative renewable energy sources [4–6]. In this context, anaerobic digestion ranks among the most important platforms for a sustainable energy production, representing a cost-effective treatment of organic residues while producing renewable energy in the form of biogas [7,8]. As a matter of fact, biogas production has been consistently identified as an important alternative to reduce the current global dependence on fossil fuels [9,10]. Biogas is a metabolic byproduct of the anaerobic degradation of organic matter (carbohydrates, proteins, and lipids) performed by the synergistic activity of complex and specialized microbial communities. Although biogas composition strongly depends on the redox state of the organic matter used as a substrate and the operating conditions set in the digesters, methane (CH_4) and carbon dioxide (CO_2) are the main components with volume percentages of 50–70 and 30–50 %, respectively [7,8]. Raw biogas also contains other pollutants in trace concentrations, such as nitrogen (N_2), volatile organic compounds, hydrogen sulfide (H_2S), ammonia (NH_3) and volatile methyl siloxanes (VMS) [11–13]. Among

---

* Corresponding author at: Institute of Sustainable Processes, University of Valladolid, Valladolid 47011, Spain.
** Corresponding author.

E-mail addresses: mariarosario.rodero@uva.es (M.R. Rodero), gquijano@nextgenbiotech.us (G. Quijano).

https://doi.org/10.1016/j.jece.2024.114106
Received 22 June 2024; Received in revised form 23 August 2024; Accepted 9 September 2024

Available online 14 September 2024
2213-3437/© 2024 The Author(s). Published by Elsevier Ltd. This is an open access article under the CC BY-NC-ND license (http://creativecommons.org/licenses/by-nc-nd/4.0/).

Nomenclature

CMS	Carbon molecular sieve membranes
CTA	modified cellulose triacetate
FT	Facilitated transport
HCP	Hyper-crosslinked polymers
IL	Ionic liquids
l	Thickness of membrane separation layer
MMM	Mixed matrix membrane
MOF	Metal organic frameworks
MOP	Microporous organic polymers
Nm^3	Normalized cubic meter
P	Permeability (mol m m^{-2} s^{-1} Pa^{-1} or Barrer (10^{-10} cm^3(STP) cm cm^{-2} s^{-1} $cmHg^{-1}$))
PA	Polyamide
PEC	polyester carbonate
PEEK	polyether ether ketone
p^{feed}	Pressure in the feed (bar)
PI	Polyimide
$p^{permeate}$	Pressure in the permeate (bar)
$p_{i,j}^{feed}$	Partial pressure of the gas *i*, *j* in the feed (bar)
$p_{i,j}^{permeate}$	Partial pressure of the gas *i*, *j* in the permeate (bar)
PSf	Polysulfone
P	Permeance (mol m^{-2} s^{-1} Pa^{-1} or GPU (10^{-6} cm^3(STP) cm^{-2} s^{-1} $cmHg^{-1}$))
PIM	Polymers of intrinsic microporosity
Q^{feed}	Feed gas flowrate (m^3 h^{-1})
$Q^{permeate}$	Permeate gas flowrate (m^3 h^{-1})
$Q_{i,j}^{permeate}$	Permeate gas flowrate of the gas *i*, *j* (m^3 h^{-1})
$Q^{retentate}$	Retentate gas flowrate (m^3 h^{-1})
RE_i	Removal efficiency of the less abundant gas *i* (%)
VMS	Volatile methyl siloxanes
$x_{i,j}$	Molar fraction of the gas *i*, *j* in the permeate
$y_{i,j}$	Molar fraction of the gas *i*, *j* in the feed
$z_{i,j}$	Molar fraction of the gas *i*, *j* in the retentate
ZIF	Zeolitic imidazolate frameworks
$\alpha_{ai/j}$	Selectivity
ΔC	Concentration gradient
ΔP	Pressure gradient (bar)
ϕ	Membrane pore size (Å)
ϕ_{total}	Total feed-to-permeate pressure ratio
$\varphi_{i,j}$	Partial feed-to-permeate pressure ratio
θ	Stage cut
θ_r	Recovery degree
η_j	Recovery yield of the richest gas *j* in the retentate stream (%)

biogas trace pollutants, the removal of H_2S and VMS (biogas *purification*) is particularly important as they mediate corrosion and abrasion issues in equipment used for energy generation from biogas, such as engines, turbines, fuel cells and combined heat and power systems [12,14].

Biogas application niches in terms of biorefinery concept are amplified when CO_2 is removed and CH_4 concentrations above 95 % (v v^{-1}) are reached. This process, known as biogas *upgrading*, reduces fuel transportation costs and allows the application of the resulting methane as a vehicle fuel and its injection in natural gas networks [15]. Biogas purification and upgrading can be achieved by means of physical-chemical and biological technologies. Biological processes, such as biological methanation of CO_2 and photosynthetic processes for CO_2 removal, have emerged as a cost-effective and sustainable alternative for biogas upgrading. These processes require low chemical and energy consumption, being typically operated under ambient temperature and pressure conditions [16,17]. Biogas upgrading by biological methanation of CO_2 consists of the utilization of H_2 by hydrogenotrophic methanogens to transform CO_2 into CH_4 [18]. Photosynthetic processes for CO_2 removal, which also are capable of removing H_2S from raw biogas, are based on the use of a consortium of microalgae and bacteria to uptake these biogas pollutants [13]. Although biological systems are efficient for removing the most important biogas trace pollutants, a low removal capacity has been consistently observed for CO_2, requiring biogas retention times in the order of 20–60 min to achieve their complete removal. Such long biogas retention times imply large bioreactor volumes, which hinders their potential application at full scale [12,19,20]. On the other hand, physical-chemical technologies, such as absorption, adsorption, and membranes are commonly applied for CO_2 removal from biogas. Absorption is based on the mass transfer of CO_2 from biogas to a liquid solution, which could be water, an organic solvent, or a chemical reagent (alkanol amines or alkali aqueous solutions). Adsorption involves the transfer of biogas pollutants onto a solid porous adsorbent [16]. Membrane technology for biogas upgrading/purification involves the selective permeation of biogas pollutants, while methane remains retained [21]. Their application has been traditionally hampered by their high investment and operating costs derived from intensive demand of chemicals or the need of high temperature and pressure conditions [22,23]. Therefore, the development of cost-efficient and robust technologies for biogas purification/upgrading is still an important research niche towards consolidating the widespread use of biomethane and reduce the global dependence on fossil fuels.

Within the aforementioned physical-chemical technologies available for biogas upgrading, the use of membranes has increased exponentially in the las five years, accounting for nearly 50 % of the total biogas upgrading technologies applied in Europe in 2021 [24]. However, despite the promising future of membrane-based technologies for biomethane production, there are still critical challenges to be addressed. For instance, it is crucial to develop efficient membranes that can operate at ambient pressures while achieving high CO_2/CH_4 separation at a low cost. Additionally, there are concerns about the reduced performance of membranes during long-term operation and in the presence of acidic gases. As a result, the number of studies on membrane materials for biogas upgrading has increased exponentially in recent years. Although various studies have recently reviewed membrane processes for biogas upgrading, many focus primarily on membrane fabrication and resistance rather than on the upgrading performance of biogas mixtures or the impact of other biogas components [7,25–27]. Furthermore, some reviews lack an overview of the fundamentals of membrane technology, which is essential for a comprehensive understanding and accurate comparison of different technologies.

The central goal of this work is addressing the state-of-the-art of the fundamentals of membrane technology to attract non-specialized readers from biotechnology and environmental engineering fields towards the most recent developments of membrane technology for biogas purification and upgrading. This review provides also a comprehensive analysis and comparison of main membrane materials used for biogas upgrading, including polymeric membranes and inorganic membranes, with a particular focus on zeolites. The development of novel materials, such as polymeric matrices with permanent microporosity, and the possibility of operating membranes at temperatures and pressures close to ambient conditions are also highlighted. Moreover, the potential of membrane technology in comparison to other upgrading methods, along with the key challenges that must be addressed for the advancement and consolidation of novel membranes for biogas purification and upgrading are identified and critically discussed. To evaluate the performance of the membranes and facilitate a comparative analysis of various membrane materials, quantitative consolidated information was collected. Data, both quantitative and qualitative, were obtained from a total of 203 studies. To create an unified database, distinct categories were established for membrane materials and biogas composition. Most of the selected studies were conducted using biogas mixtures (both synthetic and real) rather than pure gas experiments, as these better reflect conditions in practice. However, in some instances, results from pure gas studies were included due to the limited availability of studies involving biogas mixtures. Studies were generally excluded from this analysis if they used pure gases or lacked key operational characteristics and performance data, which would preclude a comprehensive evaluation.

2. Fundamentals of membrane-based technologies for biogas separation

Membrane separation is a suitable technology for biogas purification and upgrading [8,27]. The features that have traditionally encouraged the application of membranes for biogas separation include: (i) their lower investment and operating cost compared to other physical-chemical technologies; (ii) their environmentally friendly nature since no chemical waste or wastewater is produced; (iii) their compact nature and easiness of transport; (iv) their modular operation and scalability when required; and (vi) their ability to recover and valorize CO_2 in many industrial applications, which enhances the cost-effectiveness of the upgrading process [28–30]. Thus, approximately 28 % of biogas processing plants worldwide already included membrane-based technologies by 2019 [31]. It is expected that this share increases in centralized plants processing biogas flowrates < 100 $Nm^3\ h^{-1}$ and even in decentralized household digesters, considering the rapid advances in membrane technology [32].

Gas separation using membranes involves three sequential steps: (i) sorption of certain molecules at the high pressure/concentration side, namely feed side; (ii) diffusion of these molecules through the membrane; and (iii) desorption at the low pressure/concentration side, namely permeate side [33]. Thus, a gas mixture fed to the membrane is divided into two main streams, a side stream enriched with permeable molecules called *permeate*, and other stream enriched with the molecules that pass much lower through the membrane known as *retentate* (Fig. 1). Specifically, membranes for biogas separation allow gases with higher solubility in polymers or small molecular size gases, such as H_2, CO_2 or H_2S (kinetic diameters of 2.89, 3.30 and 3.60 Å, respectively) to pass through the membrane, while larger size molecules or with lower solubility, such as CH_4 (kinetic diameter of 3.80 Å) are retained [23]. The mass transfer across the membrane is an irreversible process, which occurs via a pressure and/or concentration gradient that acts as the driving force for gas separation [21,34].

2.1. Gas transport mechanisms

Membranes can be divided into two main groups based on the materials used in their manufacture, namely *non-porous* and *porous* membranes. Most polymer-based organic membranes are non-porous (also known as dense membranes), and gas molecules are transported through the unoccupied spaces between polymer chains. The total space between polymer chains available for gas flow in non-porous membranes is commonly referred as the *free volume*. Instead, most inorganic membranes are made of porous materials where gas molecules are transported from the high-pressure to the low-pressure side [21,35].

Gas transport in non-porous membranes might occur by means of either in non-facilitated or facilitated transport (FT) mechanisms. The non-facilitated separation process is based on a solution-diffusion mechanism, where molecules in the high-concentration side are dissolved in the membrane material. Then the gas molecules diffuse across

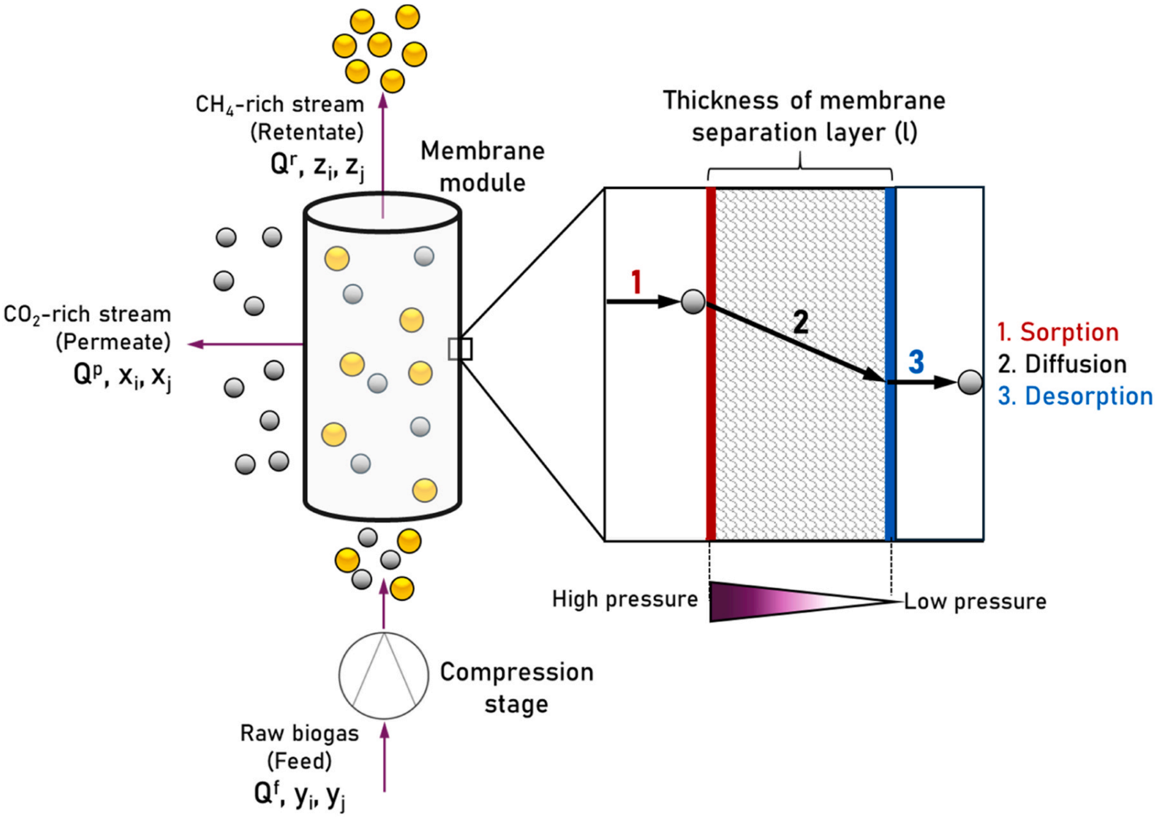

Fig. 1. Separation of the main biogas components (CH_4 and CO_2) in a membrane, illustrating the three sequential steps involved in the process. Q^f, Q^p, and Q^r stand for the gas flowrates in the feed, permeate, and retentate, respectively. Mole fractions of the *i* and *j* components in the feed, permeate, and retentate are represented by $y_{i,j}$, $x_{i,j}$, and $z_{i,j}$, respectively.

the membrane, being finally desorbed on the low-concentration side. In the solution-diffusion mechanism, the concentration difference between feed and permeate side entails a concentration gradient, whereas the pressure inside the membrane and through the membrane thickness is constant at high-pressure value but decreases rapidly on the permeate side (Fig. 2A) [4,34,36]. Instead, gas separation in FT membranes involve the following sequential steps: (i) gas sorption at the high pressure/concentration side; (ii) reversible gas reaction with a reactive component (also known as *carrier*); (iii) diffusion of reaction product (also known as *complex*) through the membrane material; (iv) dissociation of the complex and regeneration of carrier; and (v) gas release at the low pressure/concentration side [21,37]. As shown in Fig. 2A, gas transport in FT membranes can take place via a solution-diffusion mechanism where the gas-carrier complex moves freely across the membrane. However, gas jumping on fixed or mobile carriers can also occur. Carriers in non-porous membranes for CO_2 separation include amine-containing polymers, CO_2-reactive functional groups, or small reactive molecules embedded within the polymer matrix [21,37,38]. Likewise, amino acid salts and ionic liquids (IL) are some of the representative mobile carriers of FT membranes targeting CO_2 removal from biogas [7,39,40].

Gas transport in porous membranes occurs from high- to low-pressure sides through pores and the separation mechanisms mainly depend on membrane pore size (ϕ). For instance, gas separation is based on adsorption-diffusion processes (including Knudsen diffusion) at $\phi < 1000$ Å, while surface diffusion, capillary condensation, and molecular sieving occur at

$\phi < 10 - 20$ Å, $\phi < 30$ Å, and $5 < \phi < 20$ Å, respectively [41–43]. In Knudsen diffusion, gas molecules are temporarily adsorbed on the membrane surface and then reflected in a random direction [21,44]. Capillary condensation occurs when adsorbed gas compounds in inner pores condense, being only the soluble gases in this condensed gas able to flow from high to low-pressure side [42]. In molecular sieving, small molecules pass through the pores and large molecules are retained [43]. Fig. 2B depicts a summary of the mechanisms occurring during biogas separation in porous membranes.

2.2. Operating and performance parameters

In membrane-based technologies for biogas separation, the flux of permeate gas through the membrane is proportional to the pressure gradient between feed and permeate sides. In this regard, the *feed-to-permeate pressure ratio* (φ) is one of the most important operating parameters due to its influence on the molar fractions of the *i* and *j* components of the biogas mixture. Increasing the feed pressure leads to higher partial pressures of the *i* and *j* gases fed to the membrane, which ultimately promote the gas separation [45]. Hence, total and partial feed-to-permeate pressure ratios can be defined according to Eqs. 1 and 2, respectively.

$$\varphi_{total} = \frac{P^{feed}}{P^{permeate}} \tag{1}$$

$$\varphi_{i,j} = \frac{P^{feed}_{i,j}}{P^{permeate}_{i,j}} \tag{2}$$

Where P are the total pressures and $P_{i,j}$ the partial pressures of the i and j components in the feed and permeate.

High pressure gradients are achieved by maintaining $\varphi_{total} >> 1$. However, although the permeate gas flow rate is high, the less permeable gas molecules also might pass through the membrane and the purity of the permeate stream would be low. Therefore, when the gas stream in the permeate is intended to be valorized (as in the case of CO_2 from biogas), then the pressure gradient must be just high enough ($\varphi_{total} > 1$) to achieve a high purity permeate stream [46]. In practice, membranes for biogas separation can be operated under two strategies: (i) the gas mixture is introduced into the membrane using a fan at atmospheric pressure and a high-pressure gradient can be achieved by generating a negative gauge pressure (0.04 – 0.5 bar) with a vacuum pump located on the permeate side, while the retentate stream flows at ambient pressure; or (ii) the gas mixture is fed to the membrane using a compressor, the permeate stream leaves the system at ambient pressure, while the retentate stream flows at high pressure (> 4 bar) [47,48]. The second operation strategy is frequently used when the retentate stream will be further treated in another membrane module to increase its purity.

Regarding the evaluation of the membrane performance, the *stage cut* (θ) is a critical parameter that can be used to determine either the gas mixture separation or recovery degree. When the stage cut considers the fraction of the feed stream that permeates through the membrane, this parameter is a measure of the separation degree (θ_s) according to Eq. 3.

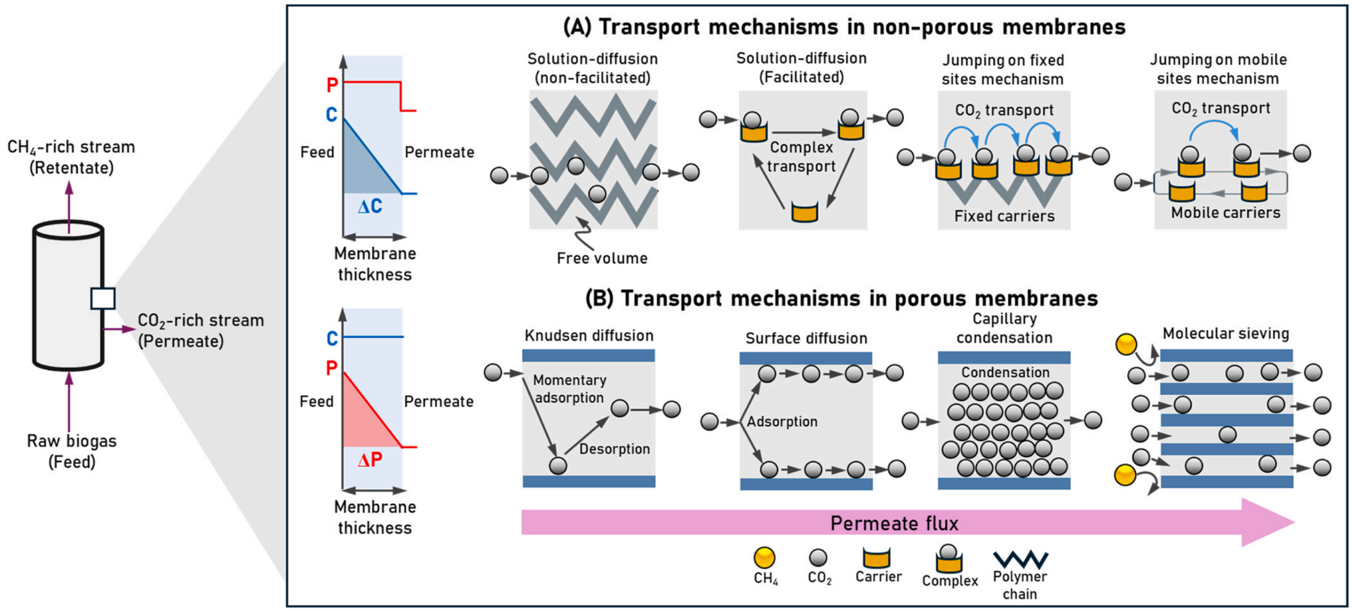

Fig. 2. Gas transport mechanisms in (A) non-porous and (B) porous membranes. C and P represent the gas concentration and pressure, while ΔC and ΔP are the corresponding gradients between the feed and permeate sides, respectively.

$$\theta_s = \frac{Q^{permeate}}{Q^{feed}} \tag{3}$$

The stage cut expresses the recovery degree (θ_r) when the retentate-to-feed flow ratio is considered (Eq. 4).

$$\theta_r = \frac{Q^{retentate}}{Q^{feed}} \tag{4}$$

A high purity permeate is achieved when θ_s is very close to zero ($\theta s \rightarrow 0$), whereas no separation is obtained if θ_s is very close to 1 [4,49,50].

The *permeance* (*P*) is a proxy of the ability of the membrane to allow specific gases to pass through the membrane, considering the permeate flowrate of the *i* or *j* gases ($Q_{i,j}^{permeate}$) across the membrane per area unit (A) due to a pressure difference between feed and permeate sides as follows:

$$\mathscr{P} = \frac{Q_{i,j}^{permeate}}{A(p_{i,j}^{feed} - p_{i,j}^{permeate})} \tag{5}$$

Permeance is a useful parameter for industrial-scale applications because it takes into consideration the membrane area. As shown in Eq. 5, if specific permeance is required, an increase of the $Q_{i,j}^{permeate}$ will imply a proportional increase of membrane area. Thus, the design of modular membrane processes should be based on this parameter [36,51]. The *membrane permeability* (P) is another performance parameter derived from the permeance, which considers the thickness of membrane separation layer (l):

$$P = \mathscr{P} \times l \tag{6}$$

Membrane permeability is useful to estimate the mass transport through the membrane, being an intrinsic material property commonly employed to compare different materials during the research and development stage. Unlike permeance, this parameter depends on the membrane thickness, which is constant and therefore cannot be used to scale the separation process [52]. The separation factor, most referred as *membrane selectivity* ($\alpha_{i/j}$), is a performance parameter obtained from the molar fractions of *i* and *j* gases on the permeate and feed sides according to Eq. 7:

$$\alpha_{i/j} = \frac{x_i / x_j}{y_i / y_j} \tag{7}$$

Where x_i and x_j are the molar fractions of the *i* and *j* components in the permeate side, while y_i and y_j correspond to molar fractions in the feed side of the membrane, respectively (see Fig. 1). The separation of the gas mixture occurs when $\alpha_{i/j} > 1$, the higher the $\alpha_{i/j}$ value, the greater the separation of gases *i* and *j*. On the contrary, no separation will occur in the membrane if $\alpha_{i/j}$ takes a value close to 1, since $x_i/x_j \approx y_i/y_j$. Most investigations on membrane-based technologies for biogas separation have reported the performance in terms of $\alpha_{i/j}$, considering only composition data in the permeate and feed streams. Nevertheless, it is quite important to characterize the retentate composition to quantify the CH_4 concentration reached.

Determining CH_4 and CO_2 concentrations in the retentate stream can be done by means of a mass balance considering the molar fractions of the *i* and *j* components in the permeate, feed, and retentate sides according to Eqs. 8–9:

$$y_i \quad Q^{feed} = (x_i Q^{permeate}) + (z_i Q^{retentate}) \tag{8}$$

$$y_j Q^{feed} = \left(x_j \quad Q^{permeate}\right) + \left(z_j Q^{retentate}\right) \tag{9}$$

The removal efficiency (RE) of the less abundant gas *i* in the retentate stream (CO_2 in biogas) can be calculated according to Eq. 10:

$$RE_i(\%) = \frac{y_i Q^{feed} - z_i Q^{retentate}}{y_i Q^{feed}} \times 100\% \tag{10}$$

Likewise, the recovery yield (η_j) of the richest gas *j* in the retentate stream (CH_4 in biogas) can be calculated according to Eq. 11, which is derived from Eq. 9:

$$\eta_j(\%) = \frac{z_j Q^{retentate}}{y_j Q^{feed}} \times 100\% \tag{11}$$

Since membranes cannot separate completely the gas mixture, a portion of the less permeable gas passes through the membrane. This fraction of the less permeable gas is called the *gas loss* and can be calculated according to Eq. 12:

$$R_j(\%) = \frac{x_j Q^{permeate}}{y_j Q^{feed}} \times 100\% \tag{12}$$

It is important to consider the complete set of performance parameters defined by Eqs. 1–7 and 10–12 to understand, evaluate, and scale membrane-based processes for biogas separation.

3. Performance of membrane-based technologies for biogas separation

3.1. Polymeric membranes for biogas purification and upgrading

Polymer-based membranes dominate the gas separation market due to their high flexibility, process reproducibility, scale-up simplicity and low manufacturing cost, which is in the range of 1.5–9 € m^{-2} and 9–45 € m^{-2} for hollow fiber and spiral wound membranes, respectively [29,49,53]. Membranes targeting CO_2 separation from biogas are commonly made of polymers, such as cellulose acetate, cellulose triacetate, polydimethylsiloxane, polysulfones, polycarbonates, polyimides, polyamides and poly(methyl pentenes) [4,28,54,55].

Flat-sheet and tubular membranes are also commercially available configurations for biogas separation. Flat-sheet membranes can be classified either as plate-and-frame or spiral wound type, whereas tubular membranes are commonly classified according to their internal diameter as hollow fiber (< 0.5 mm), capillary (1–3 mm) and tubular membranes (5–25 mm) [36,45] (Fig. 3). These membranes are typically arranged within a frame (*i.e.*, a stainless-steel tube) commonly known as the membrane module. The larger the number of fibers or films packed into the module, the larger the contact area between gas and membrane, but at the same time a higher volume of module is required. Hollow fiber membrane modules are usually preferred for biogas separation purposes since this configuration can hold packing densities up to ~100, ~33, ~10, and ~8 times higher compared to plate-and-frame, tubular, spiral wound, and capillary modules, respectively (Table 1) [8,48,56].

Regarding the materials, polysulfone (PSf) is the benchmark for biogas separation in polymeric membranes. This is mainly due to its robustness and ability to operate under a wide range of pressure (1 – 10 bar), temperature (5 – 40 °C), and feed gas composition (CO_2:CH_4 30–45:55–70 % v v^{-1}). When dealing with small biogas flowrates in the feed (*i.e.*, 0.09–0.18 m^3 h^{-1}), PSf membranes with a surface of 1.4 m^2 can deliver CH_4 concentrations of up to 96 % in the retentate stream with single-stage processes [57]. However, when dealing with biogas flowrates in the order of 100 Nm^3 h^{-1}, three-stage processes were required to achieve a CH_4 concentration above 98 % in the retentate stream using PSf membranes with 40 m^2 of effective area [58]. CO_2/CH_4 selectivity values of approximately 30 have been reported in the absence of H_2S. Polyimide (PI) is another commercial polymeric material used for biogas separation at temperatures ranging from 30 to 55 °C, which support a performance comparable to that observed in PSf membranes ($\alpha_{CO2/CH4}$ up to 30 and CH_4 concentrations in the retentate stream up to 99 %). The best performance of PI membranes has been reported at feeding pressures of 10–13 bar, slightly higher than the pressures

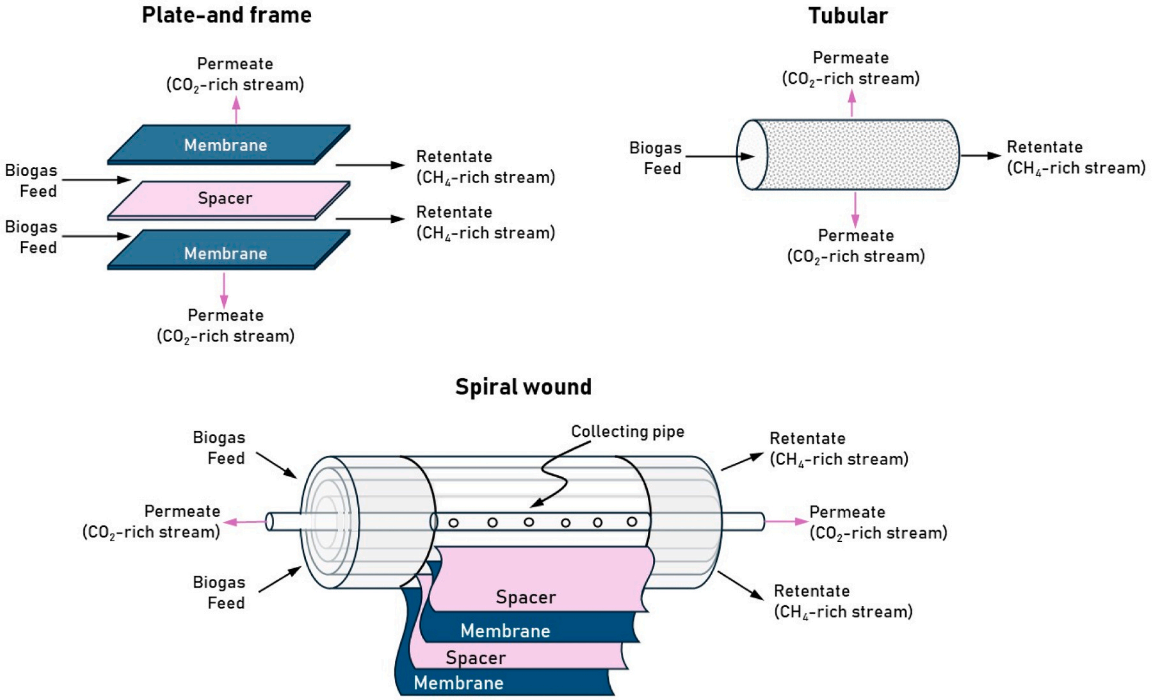

Fig. 3. Detailed structure of the main membrane configurations (plate and frame, tubular and spiral wound) used for biogas separation.

applied in PSf membranes. Even when PI membranes have been successfully tested with raw biogas, several authors recommend the previous removal of H_2S and NH_3 before CH_4/CO_2 separation [4,59,60].

Membrane modules based on polyester carbonate (PEC) and polyether ether ketone (PEEK) have also been tested for biogas separation at temperatures between 17 and 35 ºC, yielding CH_4 concentrations of 80–98 % v v^{-1} in the retentate. However, feeding pressure of up to 25 bar are required in PEEK membranes to achieve CH_4 concentrations of 98 % v v^{-1} in a single-stage process [62–64]. Interestingly, some studies have shown that membrane modules based on PSf, PI, and PEC materials can remove H_2S from biogas at efficiencies between 55 % and 89 % [6,62,65]. Wet biogas separation (moisture levels of 85–100 %) has been successfully performed in polyamide (PA) membranes under feeding pressures of 2–5 bar and temperatures between 21 and 37 ºC. However, CH_4 concentrations in the range of 79.6–91.3 % v v^{-1} are obtained in the retentate streams of PA membranes, which represents a lower performance compared to other polymeric materials in single-stage processes [65,66]. There is a trade-off between selectivity and permeability in most polymeric membranes because more permeable polymers are less selective and vice versa [41,67,68]. This phenomenon has been attributed to the increase of membrane free volume mediated by dissolved CO_2, which swells the space between polymer chains and enhances CH_4 flux though the membrane [7,69]. Consequently, a single-stage membrane separation process might achieve either maximum recovery or maximum purity, but not both [50,58]. For this reason, 2- or 3-stage membrane separation processes are required to grant CH_4 concentrations $\geq$ 91.8 % v v^{-1} and CH_4 recoveries $\geq$ 94 % in the retentate stream (Table 1). On the other hand, implementing more than 3 separation stages will compromise the economic and technical feasibility of the process because: (i) permeates must be re-compressed for its entry in subsequent separation stages, (ii) need for re-adjustment of the feeding flowrate after the first stage, and (iii) need for controlling the stage cut in each membrane module [70].

Considering natural gas processing, cellulose acetate membranes dominate the market with approximately 80 % of all installed polymeric membrane systems at full scale [71,72]. Cellulose acetate membranes require feeding pressures $\geq$ 40 bar and dry gas streams to deliver CH_4 recovery yields $\geq$ 90 % [29]. These high-pressure requirements also entail higher investment, operating, maintenance costs, which has traditionally discouraged the use of cellulose acetate membranes for biogas separation purposes in small- and medium-size biogas production plants. Therefore, the development of new polymeric membranes with a high biogas separation efficiency at pressures $\leq$ 5 bar is a critical research niche for broadening the use of membranes in small- and medium-size biogas production plants. Further drawbacks of polymeric membranes for biogas separation processes include: (i) deteriorated performance under long-term operation at high pressure and temperature; (ii) swelling, compaction and/or aging issues when operated in the presence of acidic gases; and (iii) plasticization at high CO_2 pressures [7,41,73,74]. In addition, there is still a lack of systematic studies evaluating the performance of polymeric membranes in long-term biogas separation processes. To the best of the authors' knowledge, only one study reported the stability of a PEC membrane for biogas separation during three months of operation, which highlights the need for more investigations on this regard [62].

3.2. Inorganic membranes for biogas purification and upgrading

The main characteristics of membranes based on inorganic materials include: (i) high selectivity and permeability performance; (ii) thermal and mechanical stability; (iii) resistance to erosion, bacterial degradation, and harsh conditions; and (iv) stable performance over long-term operation [49,75]. However, these membranes are also characterized by a high manufacturing cost, being prone to defects such as pinholes and surface cracks, especially when manufacturing large surface areas [72,76]. Inorganic membranes can be classified into two types: non-porous or dense ($\phi < 0.5$ nm) and porous membranes ($\phi > 0.5$ nm). Porous membranes are further categorized based on their pore size into microporous ($0.5 < \phi < 2$ nm), mesoporous ($2 < \phi < 50$ nm) and macroporous ($\phi > 50$ nm) [77].

Dense inorganic membranes can be based on palladium (and palladium alloys), perovskites, and zirconia (Fig. 4). As far as the authors know, the application of non-porous inorganic membranes for biogas separation is still unexplored. This can be explained by the fact that non-

Table 1

Performance of polymeric membranes for biogas separation under different operating conditions, where T: temperature; Q^{feed}: feed gas flowrate; p^{feed}: pressure in the feed; $[CH_4]_R$: CH_4 concentration in the retentate stream; η_{CH4}: CH_4 recovery yield in the retentate; $\alpha_{CO2/CH4}$: membrane selectivity; θs: stage cut.

Material	Module configuration	Stages	Biogas type and composition (%v v^{-1})	T (°C)	Q^{feed} (m^3 h^{-1})	p^{feed} (bar)	$[CH_4]_R$ (%v v^{-1})	η_{CH4} (%)	$\alpha_{CO2/CH4}$	θ_s	Reference
PSf	Hollow fiber	1	Dry synthetic gas CO_2:CH_4 45:55	20	0.09–0.18	1.1	96	48	^{2}1.9	0.73	[57]
PSf	Hollow fiber	1	Dry synthetic gas CO_2:CH_4:H_2S 30:69.81:0.19	25	0.003	2	84	45	^{2}1.3	0.44	[6]
PSf	Hollow fiber	1	Dry synthetic gas CO_2:CH_4 30:70	25	NR	10	95	75.3	NR	0.45	[58]
PSf	Hollow fiber	1	Dry synthetic gas CO_2:CH_4 30:70	25	NR	6	95	49	NR	0.64	[58]
PSf	Hollow fiber	3	Raw biogas CO_2:CH_4 27.5:72.5	5–25	100	10	98.8	99.1	NR	0.3/0.49/0.53	[58]
PI	Hollow fiber	2	Dry synthetic gas CO_2:CH_4:H_2O 48.1:48.1:3.8	25–50	NR	1–13	99.1	95.8	NR	0.36/0.45	[4]
PI	Hollow fiber	1	Dry synthetic gas CO_2:CH_4 30:70	NR	0.1	9	90	^{3}64.3	NR	0.5	[61]
PI	Hollow fiber	1	Raw biogas CO_2:CH_4:H_2S 30:69.998:0.002	NR	0.1	9	85	^{3}60.7	NR	0.5	[61]
PI	Hollow fiber	1	Dry synthetic gas CO_2:CH_4 20:80	30	NR	12.3	93.8	77.4	7.0	0.34	[59]
PI	Hollow fiber	1	Raw biogas CO_2:CH_4:N_2 19.8:70:9.2	30	NR	4.3	80.7	76	8.9	0.34	[59]
PEC	Hollow fiber	1	Raw biogas CO_2:CH_4:H_2S 38.9:51:0.095	35	54	7	96	69.4	3.3	NR	[62]
PEC	Hollow fiber	2	Raw biogas CO_2:CH_4:H_2S 50.7:49.1:0.14	17	54	7	96	95.6	22.9	NR	[62]
PEEK	Hollow fiber	1	Raw biogas CO_2:CH_4:N_2 44.6:54.4:1	25	96 kg/h	25*	98	40	NR	^{1}0.78	[63]
PEEK	Hollow fiber	1	Raw biogas CO_2:CH_4:H_2S:H_2:N_2 40.2:53.5:0.2:3:3.1	NR	41 kg/h	7.8	80	61	^{2}2.9	^{1}0.69	[64]
PA	Flat-sheet	1	Wet synthetic gas CO_2:CH_4:H_2S 46.6:53.3:0.1	37	0.002	2.2	79.6	^{3}77.9	^{2}3.3	^{1}0.48	[65]
PA	Flat-sheet	1	Wet synthetic gas CO_2:CH_4:H_2S 46.6:53.3:0.1	37	0.002	5	68.1	^{3}96.6	^{2}15.1	^{1}0.24	[65]
PA	Flat-sheet	1	Wet synthetic gas CO_2:CH_4 10:90	21	0.0018	5	91.3	^{3}96.0	^{2}19.7	^{1}0.49	[66]
PA	Flat-sheet	1	Wet synthetic gas CO_2:CH_4 46.2:53.8	21	0.0019	2.2	79.6	^{3}77.2	^{2}3.37	^{1}0.52	[66]

NR: not reported. PSf: polysulfone; PI: polyimide; PEC: polyester carbonate; PA: polyamide; PEEK: polyether ether ketone. *Corresponds to pressure gradient and not to feed pressure. Super indexes 1, 2 and 3 indicate that these parameters were calculated with Eqs. 3, 7 and 11, respectively.

porous inorganic membranes are prone to deteriorate in the presence of CO_2 and require up to 600 °C to achieve a high permeate flux, limiting therefore their application for biogas separation [78]. Porous inorganic membranes can be made from various materials, including metal, ceramic, glass, zeolite, and carbon molecular sieves (CMS) (Fig. 4). The structure of metallic membranes comprises a layer of fine metal powder deposited on a permeable support. Ceramic membranes are composed of macroporous layers (usually α-Al_2O_3), one or two intermediate mesoporous layers and a microporous top layer, which is actually the selective separation layer [45,79]. Glass membranes are made of calcined silica (SiO_2), a material that is highly permeable to small gas molecules like H_2, however, this material presents a limited permeance for larger molecules such as CO_2, being of poor interest for biogas separation purposes [80]. Zeolites are crystalline oxides composed of silicon (Si) and/or aluminum (Al). Membranes based on zeolites, such as chabazite (CHA), deca-dodecasil 3 rhombohedral (DDR), erionite (ERI), aluminophosphate-eighteen (AEI), lynde type A (LTA) can separate molecules like CO_2 from CH_4 in biogas streams since their average pore size is below 0.43 nm. Thus, zeolites are among the most promising materials for CO_2/CH_4 separation [74,81]. CMS membranes are manufactured by thermal decomposition of polymeric precursors such as polyacrylonitrile (PAN), cellulose triacetate, phenol formaldehyde, polyimides and poly (furfural) alcohol at temperatures commonly ranging from 600 to 800 °C [35,72]. Their high surface area and uniform

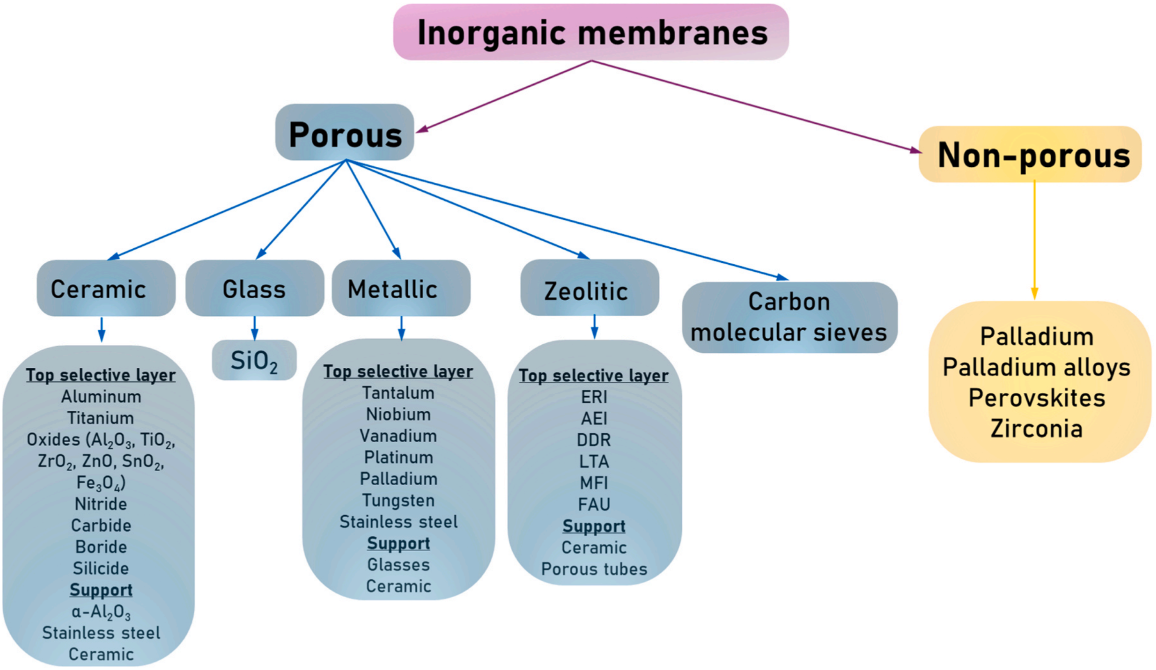

Fig. 4. General classification and materials of inorganic membranes for biogas separation.

microporosity make them suitable for biogas upgrading applications [82].

Most studies on biogas separation using inorganic membranes have reported the use of zeolites to achieve CO_2 removal (Table 2). Zeolite-based membranes are highly affine for CO_2, which facilitates its adsorption on the surface [83,84]. The CO_2/CH_4 separation in zeolite membranes is achieved by the slight difference in the molecular sizes of both molecules [85,86]. For instance, CHA-type zeolites including SAPO-34 (silicoaluminophosphate CHA type) and SSZ-13 (high silica CHA), and DDR-type zeolites such as DD3R (all-silica decadodecasil 3R) and ZSM-58, among others are particularly attractive for CO_2/CH_4 separation [75]. SAPO-34 membranes are highly selective for CO_2/CH_4 separations ($\alpha_{CO2/CH4}$ ranging from 94 to 166) due to their higher affinity for CO_2 and their pore size (0.38 nm), which matches the kinetic diameter of CH_4 [87]. Even though the separation performance of SAPO-34 membranes decreases at high pressures, selectivity values as high as 50 have been reported at 40 bar [88]. Interestingly, even when the material SAPO-34 has a low Si/Al ratio, it can tolerate small concentrations of water vapor in the feed, being therefore useful for biogas separation under more realistic conditions [89,90]. Despite their high separation performance, SAPO-34 membranes typically have a thickness ranging from 2 to 5 μm, which results in CO_2 permeances of $1{\bullet}10^{-7}$-$1{\bullet}10^{-6}$ mol m^{-2} s^{-1} Pa^{-1}. SSZ-13 membranes are simpler and present better stability in humid and chemical environments than SAPO-34 membranes due to their high Si/Al ratio [55,86]. However, although high selectivity values have been reported in some studies (up to 406) due to its ideal pore size pore size of 0.37 nm x 0.42 nm, the CO_2 permeance ($1.8{\bullet}10^{-8}$ – $4.6{\bullet}10^{-7}$ mol m^{-2} s^{-1} Pa^{-1}) is typically lower than in the case of SAPO-34 membranes. Nevertheless, the synthesis of thin membranes (0.4–1.4 μm) has increased the CO_2/CH_4 separation performance of these membranes, with CO_2 permeances of up to $4.8{\bullet}10^{-6}$ mol m^{-2} s^{-1} Pa^{-1} [89,91]. Pure silica CHA, also known as *all-silica CHA*, is a better alternative than SSZ-13 and SAPO-34 due to its hydrophobic framework, which results in an outstanding stability and inertness. Also it exhibits even higher CO_2 permeances ($1.0{\bullet}10^{-7}$ – $4{\bullet}10^{-6}$ mol m^{-2} s^{-1} Pa^{-1}) with membrane thickness (0.4–8 μm) and an adequate CO_2/CH_4 selectivity (29−150) (Table 2). However, its preparation is challenging since it requires the use of fluoride-containing dry gel, which is non-homogeneous and leads to high waste production [85].

On the other hand, DDR is a zeolite known for its high thermal, humid, and chemical stability, similar to that of pure silica CHA, but with a slightly smaller window opening (0.36 nm x 0.44 nm). As a result, high CO_2/CH_4 selectivity values have been achieved at low temperatures and pressures (105−540). Although the presence of water, along with high temperatures and pressures, can reduce membrane performance, selectivity values greater than 55 have still been reported (Table 2). Typical thicknesses of 4–10 μm have been reported, which result in typical CO_2 permeances in the order of 10^{-8} – 10^{-7} mol m^{-2} s^{-1} Pa^{-1}. Despite the advantages, synthesizing high-performance DDR membranes is challenging due to the formation of impurity phases and cracks, and they are still in the developmental stage [90,92]. In this regard, impurities were avoided in ZSM-58 membranes, although further research is still required [92].

Other zeolites, such as aluminophosphates AlPO-18 (AEI-type, 0.38 nm pore size) and AlPO-17 (ERI-type, 0.36 nm x 0.51 nm), SAPO-17 (ERI-type), mordenite framework inverted (MFI) and LTA have been reported as good candidates for CO_2 separation from biogas [93–95]. Overall, hydrophilic zeolite membranes such as AlPO-18, AlPO-17 and SAPO-17 have a low Si/Al ratio and display a poor moisture resistance, but these materials have been reported to exhibit acceptable CO_2/CH_4 selectivity values (25−101) and CO_2 permeances ($1.8{\bullet}10^{-7}$ – $1.1{\bullet}10^{-6}$ mol m^{-2} s^{-1} Pa^{-1}) at pressures below 3 bar with dry synthetic biogas. The ellipsoidal-shaped pores of ERI-type membranes result in a higher CO_2 affinity compared to spherical pores, leading to improved CO_2/CH_4 separation performance [94]. MFI membranes have a larger pore size (0.55 nm) compared to other zeolites, resulting in higher CO_2 permeances ($7{\bullet}10^{-6}$ – $1{\bullet}10^{-5}$ mol m^{-2} s^{-1} Pa^{-1}) but lower CO_2/CH_4 selectivity values (2.5–7.1). CO_2 permeances decrease with lower temperatures and Si/Al ratios. Conversely, selectivity increases as the temperature decreases [96]. Although LTA membranes can be synthetized by green and low-cost methods, their biogas upgrading performance is lower in comparison with other inorganic membranes (CO_2 permeances of $3.5{\bullet}10^{-7}$ mol m^{-2} s^{-1} Pa^{-1} and $\alpha_{CO2/CH4}$ of 16–22). It must be remarked that the maximum selectivity values reported for zeolitic membranes tested with wet synthetic biogas were approximately 50 % lower than the best selectivity achieved under dry conditions, highlighting the relevance of moisture on the resulting biogas separation performance.

Table 2

Performance of inorganic membranes (zeolites) for biogas separation under different operating conditions, where T: temperature; Q^{feed}: feed gas flowrate; p^{feed}: pressure in the feed; $\alpha_{CO2/CH4}$: membrane selectivity.

Material	Support	Biogas composition (% v v^{-1}) CO_2:CH_4	T (ºC)	Q^{feed} (m^3 h^{-1})	p^{feed} (bar)	$\alpha_{CO2/CH4}$	CO_2 permeance (mol m^{-2} s^{-1} Pa^{-1})	Reference
SAPO−34	α-Al_2O_3	50:50 (dry synthetic gas)	25	0.48	*2	129	1.0×10^{-5}	[97]
SAPO−34	α-Al_2O_3	50:50 (dry synthetic gas)	RT	NR	*1.4	152	3.9×10^{-6}	[98]
SAPO−34	α-Al_2O_3	50:50 (dry synthetic gas)	25	0.048	2	160	1.2×10^{-6}	[99]
SAPO−34	α-Al_2O_3	50:50 (dry synthetic gas)	22	1.2	1.4–40	50–162	$1.6 \times 10^{-6} – 5.3 \times 10^{-6}$	[88]
SAPO−34	α-Al_2O_3	50:50 (dry synthetic gas)	22	0.06	*2	94	1.3×10^{-6}	[87]
SSZ−13	α-Al_2O_3	50:50 (dry synthetic gas)	25	0.12	*2	70	4.6×10^{-7}	[100]
SSZ−13	Tubular porous ceramic	50:50 (dry synthetic gas)	20	0.18	1.4	180	2.8×10^{-6}	[91]
SSZ−13	α-Al_2O_3	50:50 (dry synthetic gas)	30	0.036	2	183	3.1×10^{-7}	[85]
SSZ−13	α-Al_2O_3	50:50 (dry synthetic gas)	25	0.24	2	303	1.2×10^{-6}	[55]
SSZ−13	α-Al_2O_3	50:50 (wet synthetic gas)	125	0.24	2	55	2.8×10^{-7}	[55]
SSZ−13	α-Al_2O_3	50:50 (dry synthetic gas)	25	0.006	1	64	1.8×10^{-8}	[101]
SSZ−13	α-Al_2O_3	50:50 (wet synthetic gas)	25	0.006	1	205	$3.0\times 10^{-7} – 4.0 \times 10^{-7}$	[101]
SSZ−13	Tubular porous ceramic	50:50 (dry synthetic gas)	20	NR	*1.4	116	$1.4 \times 10^{-6} – 3.4 \times 10^{-6}$	[86]
SSZ−13	Mullite tubes	50:50 (dry synthetic gas)	25	NR	*2	406	2.9×10^{-7}	[102]
SSZ−13	α-Al_2O_3	50:50 (wet synthetic gas)	50	0.006	1	44	1.0×10^{-7}	[103]
SSZ−13	Mullite tubes	50:50 (dry synthetic gas)	30	NR	2	300	2.0×10^{-7}	[104]
SSZ−13	Tubular porous ceramic	50:50 (dry synthetic gas)	RT	NR	1.4	150	4.8×10^{-6}	[89]
Si-CHA	α-Al_2O_3	50:50 (dry synthetic gas)	25	0.18	1	130	4.0×10^{-6}	[105]
Si-CHA	α-Al_2O_3	50:50 (dry synthetic gas)	20	0.12	2.4	150	2.5×10^{-6}	[106]
Si-CHA	α-Al_2O_3	50:50 (dry synthetic gas)	30	0.006	1	29	1.0×10^{-7}	[107]
DD3R	α-Al_2O_3	50:50 (dry synthetic gas)	RT	0.12	7–31.3	55–300	0.9×10^{-8} - 3.2×10^{-8}	[74]
DD3R	α-Al_2O_3	50:50 (dry synthetic gas)	RT	0.36	31.3	105	1.2×10^{-8}	[74]
DDR	α-Al_2O_3	64:36 (dry synthetic gas)	45	NR	30	182	6.6×10^{-13}	[83]
DDR	Porous silica	50:50 (dry synthetic gas)	30	0.0036	1	540	2.8×10^{-7}	[108]
DDR	Porous silica	50:50 (wet synthetic gas)	150	0.0036	1	320	3.2×10^{-7}	[108]
DDR	α-Al_2O_3	50:50 (dry synthetic gas)	20	NR	*1.4	150	8.6×10^{-7}	[90]
DDR	α-Al_2O_3	50:50 (wet synthetic gas)	20	NR	*1.4	80	2.1×10^{-7}	[90]
DDR	Porous silica	50:50 (dry synthetic gas)	25	NR	*1.4	200	4.2×10^{-7}	[76]
DDR	Porous silica	50:50 (wet synthetic gas)	80	NR	1.4	88	0.9×10^{-7}	[76]
DDR	α-Al_2O_3	50:50 (dry synthetic gas)	25	0.048	3	334	4.5×10^{-8}	[109]
DDR	α-Al_2O_3	50:50 (dry synthetic gas)	25	0.048	*1	500	3.5×10^{-8}	[109]
DDR	α-Al_2O_3	50:50 (wet synthetic gas)	30	0.048	3	300	3.6×10^{-8}	[109]
DDR	α-Al_2O_3	90:10 (dry synthetic gas)	24	0.0024	2	92	1.8×10^{-7}	[110]
DDR	α-Al_2O_3	10:90 (dry synthetic gas)	24	0.0024	2	62	1.8×10^{-7}	[110]
ZSM−58	α-Al_2O_3	50:50 (dry synthetic gas)	25	0.09	3	290	1.7×10^{-7}	[92]

(continued on next page)

Table 2 (*continued*)

Material	Support	Biogas composition (% v v^{-1}) CO_2:CH_4	T (°C)	Q^{feed} (m^3 h^{-1})	p^{feed} (bar)	$\alpha_{CO2/CH4}$	CO_2 permeance (mol m^{-2} s^{-1} Pa^{-1})	Reference
AlPO−18	Mullite tubes	50:50 (dry synthetic gas)	30	0.45	*2	93	9.2×10^{-7}	[95]
AlPO−18	α-Al_2O_3	50:50 (dry synthetic gas)	RT	NR	*1	101	1.8×10^{-7}	[111]
AlPO−17	α-Al_2O_3	50:50 (dry synthetic gas)	25	0.48	3	25–31	5.0×10^{-7}	[94]
SAPO−17	Mullite tubes	50:50 (dry synthetic gas)	25	0.48	3	50–53	1.1×10^{-6}	[94]
MFI	α-Al_2O_3	50:50 (dry synthetic gas)	−24	0.48	7	7.1	6.8×10^{-6}	[96]
MFI	α-Al_2O_3	50:50 (dry synthetic gas)	27	0.48	7	2.5	1.0×10^{-5}	[96]
MFI	α-Al_2O_3	50:50 (dry synthetic gas)	22	NR	6	6.2	7.0×10^{-6}	[112]
LTA	clay-Al_2O_3	45:55 (dry synthetic gas)	30	0.012	1–3	16–22	3.5×10^{-7}	[113]

* Corresponds to pressure gradient and not to the feed pressure. NR: not reported. RT: room temperature; AlPO: aluminophosphate; α-Al_2O_3: alumina; CHA: chabazite; DDR: deca-dodecacil 3 rhombohedral; DD3R: all-silica decadodecasil 3R; LTA: lynde type A; MFI: mordenite framework inverted; SAPO: silico-alumino phosphate; SSZ: high-silica aluminosilicate zeolite; ZSM: zeolite socony mobil.

CMS membranes have shown to be efficient in separating gases through molecular sieving, but generally require working pressures ≥ 10 bar, being applied in natural gas sweetening processes [73]. Although CMS membranes are both permeable and selective, their use for biogas separation applications are scarce in the literature. Selectivity values of 59 and 103 have been reported for CMS membranes obtained from the pyrolysis of polyimides at 800 °C [114,115]. Likewise, a selectivity of 195 was achieved with a CMS membrane obtained from the thermal degradation of cellulose acetate at 600 °C [73]. However, pressures of up to 4–10 bar are required to achieve such high selectivity values, which has limited the application of these membranes in small- and medium-size biogas production facilities.

Porous inorganic membranes can operate at relatively low temperature (20 and 35 °C) and pressure conditions (1–7 bar), supporting an effective transport mechanism compared to polymeric membranes. In this regard, CMS and zeolite-based membranes are good candidates for biogas upgrading. However, the massive production of defect-free materials and the effective testing of these membranes at full-scale conditions constitute two major challenges to overcome towards the consolidation of these membranes for biogas separation [72,114]. Even when the research on zeolitic membranes for CO_2/CH_4 separation has been extensive, their high manufacturing costs and the poor material reproducibility represent additional obstacles to tackle [106,116]. For instance, the manufacturing cost of DDR zeolite membranes is approximately 3000 € m^{-2}, while the cost of conventional hollow fiber polymeric membranes is typically ∼ 150 times lower [33]. Hence, reducing the manufacturing costs of porous inorganic membranes for biogas separation would enhance their chances for massive application in small- and medium-size biogas production plants.

3.3. Next-generation membranes for biogas purification and upgrading

As discussed in previous sections, the main limitations of polymeric membranes for biogas separation include plasticization and degradation at high feed pressures and/or partial pressures of CO_2 (4–40 bar), with the subsequent performance decrease [42,114]. The following strategies have been proposed to overcome these problems: (i) polymer crosslinking, (ii) polymer annealing, (iii) blending of high-performance polymers, (iv) thermal and chemical modifications of polymers, (v) development of composite membranes, and (vi) particle filling. These strategies have also been proposed to avoid or minimize faulty manufacturing and improve membrane reproducibility [7,69].

Copolymerization and blending are two techniques applied for the manufacturing of membranes with non-facilitated transport, which enhance mechanical and durability properties [45]. Blending rubbery polymers with higher CO_2 permeabilities and glassy polymers with higher CO_2/CH_4 selectivity has been demonstrated to improve separation properties and prevent plasticization [117]. A blended mixture of modified cellulose triacetate (CTA) with 6 % PSf resulted in an ideal CO_2/CH_4 selectivity of 30.7 and a permeability of 11.1 Barrer at 4 bar and 25°C. This selectivity value was higher than those obtained for the membranes of pure PSf or CTA, with a permeability slightly lower than that of CTA (13.5 Barrer) [118]. Additionally, the blended polyetherimide-polyvinylacetate membranes have shown better separation performance compared to pure polymer membranes [119]. However, some of the studies have been tested with pure gases, making it necessary to test them with synthetic mixtures and real biogas. As shown in Table 3, polyimide ranks among the most studied materials for the manufacture of polymeric non-porous membranes targeting biogas separation. Fluorinated polyimide containing 6FDA (4,4′-(Hexafluoroisopropylidene) diphthalic anhydride) is an attractive material for CO_2/CH_4 separation since the presence of a $C(CF_3)$ group increases the membrane free volume, and consequently, the CO_2 permeability [120]. Overall, polyimides incorporating the 6FDA might support CO_2/CH_4 selectivity values between 30 and 94 and CO_2 permeabilities of 10–120 Barrer at pressures ranging from 4 to 14 bar [71,121,122]. Additionally, copolymers containing 6FDA were tested with gas mixtures that included H_2S. The presence of H_2S did not significantly diminish CO_2/CH_4 separation efficiency, with H_2S/CH_4 selectivities reported up to 23 [123]. However, high H_2S concentrations (9.95 % v v^{-1}) caused plasticization and deviations in separation performance [124]. Thermal annealing can improve the membrane's stability against H_2S, but further enhancements, such as crosslinking stabilization, are recommended to optimize performance in streams with high H_2S concentrations.

In the last decade, research efforts have been focused on the development of polymeric matrices with permanent microporosity (*i.e.*, $\phi <$ 2 nm), which can provide a high free volume for enhancing gas transport through membranes based on these materials [43,130]. The engineering of microporous organic polymers (MOP) as membranes, *in situ* hyper-crosslinking of aromatic non-porous polymeric membranes (HCP), thermally-rearranged polymers (TR), and the fabrication of mixed matrix membranes (MMM) are the main strategies to create permanent porosity in polymeric membranes [131,132]. Polymers of intrinsic microporosity (PIM) are a subclass of MOP with promising perspectives in the development of membranes for biogas separation [7,133] (Fig. 5). In these polymers, the gas solubility and, as a result, CO_2 permeability, are higher than in other polymers due to their microporosity [26]. Overall, the selectivity of PIM-1 (a subclass of PIM) is

Table 3
Performance of next-generation polymeric membranes based on polyimides and polymers of intrinsic microporosity for biogas separation under different operating conditions, where: T: temperature; p^{feed}: pressure in the feed and $\alpha_{CO2/CH4}$: membrane selectivity.

Membrane type	Polymer matrix	Biogas composition (%v v^{-1}) CO_2:CH_4	T (°C)	p^{feed} (bar)	$\alpha_{CO2/CH4}$	CO_2 permeability (Barrer)	Reference
Blended polymers	6FDA-DAT1/6FDA-DAT2	50:50 (dry synthetic gas)	35	4	30–38	90–120	[121]
Blended polymers	Matrimid®/F-SPEEK	10:90 (dry synthetic gas)	25	10	47	33.2	[125]
Blended polymers	PSf/CTA	Pure gas (CO_2 and CH_4)	25	4	31	12.1	[118]
Blended polymers	PEI/PVAc	Pure gas (CO_2 and CH_4)	RT	2	30	NR	[119]
Copolyimides	6FDA-DAM-DABA	CO_2:CH_4:H_2S 19.9:70.15:9.95 (dry synthetic gas)	35	6	49	NR	[124]
Block copolyimides	6FDA-mPDA−6FDA-durene	CO_2:CH_4:N_2:H_2S 10:59:30:1 (dry synthetic gas)	22	34.5	37	19	[123]
Crosslinked copolyimides	6FDA-DAM-DABA	50:50 (dry synthetic gas)	22	13.8	44	NR	[122]
Hydroxyl-functionalized-FTM	TPDA-APAF	50:50 (dry synthetic gas)	35	4	61	39	[114]
Hydroxyl-functionalized-FTM	TPDA-ATAF	50:50 (dry synthetic gas)	35	4	34	37	[114]
Hydroxyl-functionalized-FTM	6FDA-DAP/6FDA-DAR	50:50 (dry synthetic gas)	35	4	92–94	7.5–10.5	[71]
Hydroxyl-functionalized-FTM	6FDA-mPDA	50:50 (dry synthetic gas)	35	4	70	15	[71]
Amidoxime-functionalized-FTM	AO-PIM−1	50:50 (dry synthetic gas)	35	2	24	850	[126]
CMS membrane	PIM−6FDA-OH	50:50 (dry synthetic gas)	35	10	59	471	[127]
CMS membrane	6FDA-DETDA-DABA	50:50 (dry synthetic gas)	35	4.1	102.7	1397	[115]
Composite membrane	PVC-Pebax 1657	50:50 (dry synthetic gas)	25	5	28	155	[128]
Composite membrane	Matrimid®/NHs−20	30:70 (dry synthetic gas)	30	10	86	250	[129]
PIM	PIM−1	50:50 (dry synthetic gas)	35	2	13	5600	[126]
Thermally-rearranged-FTM	PIM−6FDA-OH	50:50 (dry synthetic gas)	35	10	15	557	[127]

NR: not reported. AO: amidoxime-functionalized; APAF: 2,2-bis(3-amino-4-hydroxyphenyl)-hexafluoropropane; ATAF: 5,5′-(hexafluoroisopropylidene)-di-o-toluidine; CMS: Carbon molecular sieve; CTA: cellulose triacetate; DABA: 3,5-diaminobenzoic acid; DAM: diaminomesitylene; DAP: 2,4-diaminophenol-dihydroxyl; DAR: 4,6-diamino resorcinol di hydroxyl; DAT1: 2,6-diaminotriptycene; DAT2: extended iptycene diamine derivative of DAT1; DETDA: diethyltoluenediamine; Durene: 2,3,5,6-tetramethyl-1,4-phenylenediamine; F-SPEEK: Fluorinated sulfonated poly ether ether ketone; FTM: Facilitated transport membranes; mPDA: 3,3′-diamino-4,4′-dihydroxybiphenyl; NHs: Nanohydrogels; OH: hydroxyl-functionalized; Pebax = Poly(ether-block-amide); PEI: Polyetherimide; PIM: Polymer of intrinsic microporosity; PSf: Polysulfone; PVAc: Polyvinylacetate; PVC: Polyvinyl chloride; TPDA: 9,10-triisopropyl-bridgehead triptycene dianhydride; 6FDA: 4, 4′-(Hexafluoroisopropylidene) diphthalic anhydride.

relatively low (< 13). However, increasing selectivity values can be achieved at pressures lower than 4 bar by introducing nanostructures, functionalized materials, applying crosslinking, TR or blending with other polymers (Table 3). Regarding FT membranes for CO_2/CH_4 separation, composite membranes comprising two or more materials (arranged in layers) have been investigated, as well as the functionalization of high-performance polymers like PIM and 6FDA to obtain high selectivity and permeability performances.

MMM are the most promising substitutes of conventional membranes because they combine the easy processability and reasonable cost of polymers with the high flux/selectivity of inorganic materials. Such features allow MMM for: (i) increasing the membrane free volume and facilitate CO_2 transport, (ii) obtaining better thermal and chemical stability, and (iii) increasing the membrane specific area and porosity [68,134,135]. MMM result from the incorporation of a solid phase known as filler in a continuous polymer matrix. The porous fillers in MMM separate gases by molecular sieving, whereas non-porous fillers increase the space within the polymer matrix for gas molecules to be easily transported (Fig. 5). Therefore, the selectivity of small molecules is improved over larger gas molecules [136]. MMM with good CO_2 separation performance must grant a sufficient adhesion and compatibility between the polymer matrix and the filler to avoid the presence of non-selective voids that leads to high fluxes but low selectivity [137]. Inorganic porous materials, such as zeolites, and metal organic frameworks (MOFs), have been extensively studied as filler materials in MMM systems (Table 4).

Zeolites exhibits the advantage of high thermal and chemical stability. In this context, SAPO-34 has been tested as a filler material due to its suitable pore size. For instance, incorporating SAPO-34 into MMMs increased CO_2 permeability by 68 % and CO_2/CH_4 selectivity by 37 % compared to the pristine 6FDA-DAM membrane when using dry synthetic biogas [138]. However, the use of wet biogas mixtures in MMM membranes containing SAPO-34 significantly diminishes gas separation performance due to pore blockage by adsorbed water. This issue can be addressed by modifying SAPO-34 with fluorocarbons, which enhances its hydrophobicity [139]. Other zeolites, such as NaY and ZSM-5, have larger pore sizes (7.4 Å and 5.5 Å, respectively), allowing both CO_2 and CH_4 to permeate through the filler material. In this context, increasing the proportion of these fillers (5–15 %) in the membrane matrix improved CO_2 permeance and CO_2/CH_4 selectivity, likely due to the enhanced rigidity of the polymer matrix. However, higher filler concentrations led to reduced selectivity [140,141]. Other zeolites, such as 5 A, ZSM-25 and T, have also shown an increase in both CO_2 permeability and CO_2/CH_4 selectivity at temperatures of 35–40°C and

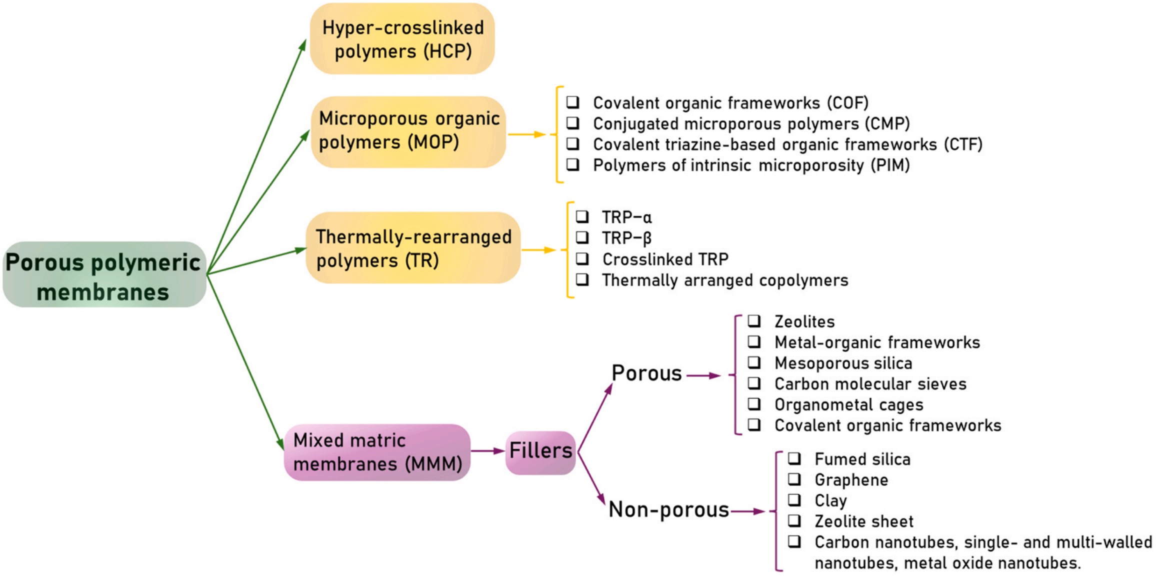

Fig. 5. Classification and characteristics of porous polymeric membranes.

pressures lower than 5 bar (Table 4). MOF is a new class of nanoporous crystalline materials that has a tremendous potential for CO_2 separation. MOF has ordered structures with strong bonds between inorganic (metal ions) and organic units (organic linkers), forming tunable porous structures with pore diameters ranging from 3 to 20 Å [142]. Additionally, MOFs exhibit a high surface area (typically between 1000 and 10,000 $m^2\ g^{-1}$), low density, and enhanced packing capacity [143]. The most commonly studied MOFs used as fillers in MMMs include Zeolitic Imidazolate Frameworks (ZIFs), which are based on metal ions with valence electrons and imidazole derivatives as linkers; Materials Institute Lavoisier (MIL), which are based on trivalent metal ions and carboxylic acid ligands and University of Oslo (UiO), which utilizes dicarboxylic acid building units, $Zr_6(\mu_3\text{-}O)_4(\mu_3\text{-}OH)$ metal precursors, and an organic linker (Table 4). ZIF-8, characterized by its porous crystalline structure, large pore size of 11.6 Å, and 6-ring window aperture of 3.4 Å, has been extensively studied as a filler for CO_2/CH_4 separation [144]. This is due to his high surface area and exceptional thermal and mechanical resistance. The incorporation of ZIF-8 into a 6FDA-copolyimide led to a 130 % increase in CO_2 permeability and a 37 % improvement in CO_2/CH_4 selectivity [145]. Another fillers gaining attention for MMM production for biogas upgrading due to their thermal stability and enhancement of CO_2/CH_4 separation performance are MIL-53 and UiO-66. A study showed that a MMM made of Matrimid/15 % MIL-53 outperformed both pure Matrimid and MMMs with zeolite ZSM-5, achieving a 270 % increase in CO_2 permeance and a 60 % increase in CO_2/CH_4 selectivity compared to pure Matrimid [140]. Additionaly, the incorporation of UiO-66 nanoparticles into 6FDA co-polyimides enhanced CO_2 permeability and CO_2/CH_4 selectivity by up to 180 % and 220 %, respectively [146].

The use of IL has been recently proposed to improve the characteristics of MMM and the CO_2 transport. The variety of IL structures and cation-anion combinations allow a wide range of materials functionalization for the manufacturing CO_2/CH_4 separation membranes [38, 190]. It must be remarked that manufacturing defect-free MMM with improved separation performance and without compromising the mechanical and thermal stability is difficult and challenging. In this regard, incorporating IL in MMM has improved mechanical characteristics of the membrane and its selectivity, offering good interfacial wetting between the filler and the polymer matrix, as well as higher CO_2 solubilization in the membrane material [189]. For instance, the incorporation of IL into a porous organic cage filler significantly improved CO_2/CH_4 selectivity by 106 % and CO_2 permeability by 16 % [188]. Metal ions of MOF might act also as CO_2 FT carriers. Thus, fillers like MOF, zeolites, and titanosilicates are usually functionalized and incorporated into polymer blends, copolymers, and PIM to manufacture MMM with facilitated CO_2 transport [121].

In general, most MMM can be successfully operated under pressures below 5 bar and temperatures ranging from 25 to 35 °C. Unfortunately, MMM have been tested under quite low biogas flowrates and, in many cases, this data is not provided. Therefore, more realistic Q^{feed} values must still be investigated in these membranes. However, the results obtained so far are very promising towards establishing MMM as the benchmark membrane technology for biogas separation since selectivity values above 100 have been obtained under low pressure and temperature conditions.

4. Implications for industrial membrane applications in biogas upgrading and purification

The use of membrane separation for upgrading biogas has considerably increased, being one of the most applied technologies in new installations. The first large-scale industrial membrane-based biogas upgrading plant in Europe for simultaneous CH_4 and CO_2 purification was built in 2016/17 by Tecno Project Industriale in Curno, Italy. It uses polyimide hollow fiber membranes, 1.3 m long with a 0.5 mm diameter. The plant can process 1250 $m^3\ h^{-1}$ of raw biogas per line across five lines, achieving a total biomethane production capacity of 3000 $Nm^3\ h^{-1}$ with a purity greater than 96 % $v\ v^{-1}$ [195]. Membrane technology is attractive due to its high CH_4 recovery and low CH_4 losses (<5 % $v\ v^{-1}$). In addition, its low energy demand (0.2–0.38 kWh Nm^{-3}) and lack of chemical use, which avoids the production of toxic compounds, are significant advantages [7]. As a result, membranes show the best environmental performance compared with other physical-chemical technologies. Specifically, the results of a life cycle impact assessment revealed that membrane exhibits a lower negative impact compared to its counterparts in terms of respiratory inorganic, global warming and non-renewable energy potential [196]. Nevertheless, the membrane option requires a greater input of energy in comparison to biological technologies, such as photosynthetic biogas upgrading (Table 5). Furthermore, the investment costs of membranes modules, mainly for medium-small facilities, remain quite high (4700–6000 € $(Nm^3\ h^{-1})^{-1}$). For higher plants, similar investment costs than other technologies have been reported (1300–2700 € $(Nm^3\ h^{-1})^{-1}$) (Table 5). Although the initial investment is high, the ongoing maintenance costs (3–4 % of

Table 4
Performance of next-generation porous polymeric membranes for biogas separation under different operating conditions, polymer matrix and filler. where T: temperature; Q^{feed}: feed gas flowrate; p^{feed}: pressure in the feed; $\alpha_{CO2/CH4}$: membrane selectivity.

Membrane type	Polymer matrix	Filler/Coater/IL	Biogas composition (%v v^{-1}) CO_2:CH_4	T (°C)	Q^{feed} (m^3 h^{-1})	p^{feed} (bar)	$\alpha_{CO2/CH4}$	CO_2 permeability (Barrer)	Reference
Zeolite-MMM	Matrimid®	5 A zeolite	50:50 (dry synthetic gas)	40	NR	*1	36	22.4	[147]
Zeolite-MMM	Matrimid®5218	NaY zeolite	10:90 (dry synthetic gas)	35	NR	2	43	10	[141]
Zeolite-MMM	Matrimid®5218	Sm-NaY zeolite	10:90 (dry synthetic gas)	35	NR	2	56	17	[141]
Zeolite-MMM	Matrimid® 5218	Li/Na-ZSM−25	35:65 (dry synthetic gas)	35	NR	5	35	8	[148]
Zeolite-MMM	6FDA-Durene	T zeolite	50:50 (dry synthetic gas)	30	NR	3.5	12	511.1	[149]
Zeolite-MMM	6FDA-Durene	Sm-T zeolite	50:50 (dry synthetic gas)	30	NR	3.5	7	550	[150]
Zeolite-MMM	6FDA-DAM	SAPO−34	50:50 (dry synthetic gas)	25	NR	*2.5	26	1552	[138]
Zeolite-MMM	PSf	SAPO−34	50:50 (wet synthetic gas)	30	NR	3.5	36	NR	[139]
Zeolite-MMM	PEI	SAPO−34	50:50 (dry synthetic gas)	30	NR	*2	79	NR	[136]
Zeolite-MMM	Matrimid	ZSM−5	10:90 (dry synthetic gas)	35	NR	3	14.1	NR	[140]
MOF-MMM	PSf	Bio-MOF−1	10:90 (dry synthetic gas)	25	0.06	10	39	14.1	[151]
MOF-MMM	Matrimid® 5218	Cu_3BTC_2	50:50 (dry synthetic gas)	35	NR	5	51	14	[152]
MOF-MMM	Pebax® 1657	Fe-BTC	10:90 (dry synthetic gas)	25	NR	7	24	220	[153]
MOF-MMM	Matrimid® 5218	Fe-BTC	50:50 (dry synthetic gas)	35	NR	5	28	12	[154]
MOF-MMM	6FDA-Durene	KAUST−7	10:90 (dry synthetic gas)	35	NR	2	62	1300	[155]
MOF-MMM	PIM−1	Mg-MOF−74	50:50 (dry synthetic gas)	25	NR	4	19.2	18000	[156]
MOF-MMM	Matrimid	MIL−53(Al)	10:90 (dry synthetic gas)	35	NR	3	20	NR	[140]
MOF-MMM	Matrimid® 5218	MIL−53(Al)	50:50 (dry synthetic gas)	35	NR	5	47	18	[152]
MOF-MMM	Pebax® 1657	MIL−101	50:50 (dry synthetic gas)	25	NR	4	49	34	[157]
MOF-MMM	PSf	MSS-Z8	50:50 (dry synthetic gas)	35	0.003	3.3	31	25	[158]
MOF-MMM	6FDA-Bisp	UiO−66	10:90 (dry synthetic gas)	35	0.003	*2	42	108	[146]
MOF-MMM	6FDA-ODA	UiO−66	10:90 (dry synthetic gas)	35	0.003	*2	57	43	[146]
MOF-MMM	6FDA-DAM	UiO−66	10:90 (dry synthetic gas)	35	0.003	*2	30.9	1912	[146]

(*continued on next page*)

Table 4 (*continued*)

Membrane type	Polymer matrix	Filler/Coater/IL	Biogas composition (%v v^{-1}) CO_2:CH_4	T (°C)	Q^{feed} (m^3 h^{-1})	p^{feed} (bar)	$\alpha_{CO2/CH4}$	CO_2 permeability (Barrer)	Reference
MOF-MMM	PSf/PI	UiO−66-GO	50:50 (dry synthetic gas)	35	0.003	3.4	51	21	[159]
MOF-MMM	Matrimid®/PEG	ZIF−8	50:50 (dry synthetic gas)	25	0.0024	8	15.4	33	[160]
MOF-MMM	Matrimid® 5218	ZIF−8	50:50 (dry synthetic gas)	35	NR	5	44	20	[152]
MOF-MMM	Matrimid®	ZIF−8/ambz	50:50 (dry synthetic gas)	35	NR	6.9	43	10	[161]
MOF-MMM	6FDA-Bisp	ZIF−8	50:50 (dry synthetic gas)	25	NR	5	37	80	[145]
MOF-MMM	6FDA-durene	ZIF−8	50:50 (dry synthetic gas)	30	NR	3.5	7.6	320	[162]
MOF-MMM	Pebax−1657	ZIF−8	20:80 (dry synthetic gas)	25	NR	2	13	NR	[67]
MOF-MMM	PU	ZIF−8	90:10 (dry synthetic gas)	35	NR	5	12.9	70	[163]
MOF-MMM	PI	ZIF−8	50:50 (dry synthetic gas)	35	NR	5	43	47	[164]
MOF-MMM	PMPS	ZIF−8	50:50 (dry synthetic gas)	RT	0.006	1.2	7	827	[165]
Amine-functionalized -MOF-MMM	Pebax	NH_2-MIL−53	20:80 (dry synthetic gas)	35	NR	22	69	159	[166]
Amine-functionalized -MOF-MMM	PI	NH_2-MIL−53(Al)	50:50 (dry synthetic gas)	25	0.006	*3	60	6	[167]
Amine-functionalized -MOF-MMM	PSf	NH_2-MIL−125(Ti)	50:50 (dry synthetic gas)	30	NR	3	29.5	29	[168]
Amine-functionalized -MOF-MMM	PIM−1	UiO−66-NH_2	52.1:47.9 (dry synthetic gas)	25	NR	1	22	4100	[169]
Functionalized-MOF-MMM	6FDA-DAM	UiO−66-NH-$COCH_3$	30:70 (dry synthetic gas)	35	NR	20	19.7	291	[135]
Functionalized-MOF-MMM	6FDA-DAM	UiO−66-NH-$COCH_3$	CO_2:CH_4:H_2S 30:65:5 (dry synthetic gas)	35	NR	20	18.2	193	[135]
Functionalized-MOF-MMM	6FDA-DAM	UiO−66-NH-$COCH_3$	50:50 (dry synthetic gas)	35	0.003	5	39	1400	[170]
Functionalized-silica-MMM	Matrimid® 9725	SO_3H-MCM−41	50:50 (dry synthetic gas)	25	NR	10	32	9	[171]
Composite membrane	PIM−1	TA	30:70 (dry synthetic gas)	30	NR	2	19	3250	[172]
Nanocomposite-MMM	Matrimid® 5218	CNTs/GO	30:70 (dry synthetic gas)	30	NR	2	84.6	38	[173]
Nanocomposite-MMM	PIM−1	CuBDC-ns	50:50 (dry synthetic gas)	25	0.003	*1	15.6	NR	[28]
Nanocomposite-MMM	PIM−1	POSS	50:50 (dry synthetic gas)	25	NR	4	12	4087	[174]
Nanocomposite-MMM	PIM−1	POSS	50:50 (dry synthetic gas)	35	NR	5	13	2400	[175]
Nanocomposite-MMM	Pebax	Ni-ns	10:90 (dry synthetic gas)	25	NR	*2	31.7	170	[176]

(*continued on next page*)

Table 4 (*continued*)

Membrane type	Polymer matrix	Filler/Coater/IL	Biogas composition (%v v^{-1}) CO_2:CH_4	T (°C)	Q^{feed} (m^3 h^{-1})	p^{feed} (bar)	$\alpha_{CO2/CH4}$	CO_2 permeability (Barrer)	Reference
Hybrid-Nanocomposite-MMM	Pebax	PEG–MWCNT	30:70 (dry synthetic gas)	22	NR	2	19	44	[177]
Functionalized-Nanocomposite-MMM	Pebax	PDA-Ag^+	30:70 (dry synthetic gas)	30	0.003	2	27	125	[178]
FT-MMM	Pebax	MCM−41	30:70 (wet synthetic gas)	25	NR	1	18	700	[179]
FT-MMM	SPEEK	b-IM@PMAA	30:70 (wet synthetic gas)	25	NR	1	74	2250	[180]
FT-MMM	SPEEK	TiO_2–DA–PEI	30:70 (wet synthetic gas)	25	NR	1	47	1620	[181]
FT-Zeolite-MMM	Pebax	PEI-MCM−41	30:70 (wet synthetic gas)	25	NR	1	40	1400	[179]
FT-Nanocomposite-MMM	SPEEK	TNT-IM	30:70 (dry synthetic gas)	25	0.0027	1	54.8	1953	[182]
FT-Nanocomposite-MMM	Pebax	GO-DA-Zn^{2+}	30:70 (dry synthetic gas)	30	NR	2	28.8	138	[183]
Titanosilicate-MMM	PI	ETS−10	50:50 (dry synthetic gas)	35	NR	8	33.3	5.8	[184]
Titanosilicate-MMM	PI	TS1–25	50:50 (dry synthetic gas)	35	NR	8	31.6	7.9	[184]
AS-MMM	Pebax® 1657	CaLS	30:70 (wet synthetic gas)	25	NR	3	29	3585	[185]
CMS-MMM	Matrimid® 9725	CMS	50:50 (dry synthetic gas)	35	NR	9	38	25	[137]
Metal oxide-MMM	Pebax® 1657	$ZnCo_2O_4$	10:90 (wet synthetic gas)	25	NR	2	31	150	[186]
IL-MMM	Pebax	[Hmim][NTf_2]@LDHN−6	10:90 (wet synthetic gas)	25	0.0051	2	34	650	[187]
IL-MMM	PIM−1	IL@CC3	50:50 (dry synthetic gas)	25	NR	2	73	7868	[188]
IL-MOF-MMM	PSf	Cu-BTC/[Bmim][Tf_2N]	50:50 (dry synthetic gas)	30	NR	4	19	NR	[189]
RTIL-MOF-MMM	PSf	ZIF−67/RTIL	50:50 (dry synthetic gas)	25	0.06	10	67	20	[5]

[*] Corresponds to pressure gradient and not to the feed pressure. NR: not reported. RT: room temperature. AS: anionic surfactant; b-IM@PMAA: polymer brushes functionalized double-shelled organic submicrocapsules; CaLS: calcium lignosulfonate; CC3: rigid porous organic cage constructed with four trialdehyde and six diamine molecules; CNTs/GO: carbon nanotubes/graphene oxide; CuBDC-ns: copper 1,4-benzenedicarboxylate nanosheets; Cu_3BTC_2: copper benzene-1, 3, 5-tricarboxylate; ETS-10: Engelhard Corporation titanosilicate; Fe-BTC: iron 1,3,5-benzenetricarboxylate; F-SPEEK: fluorinated sulfonated poly(ether ether ketone); GO-DA-Zn^{2+}: zinc ion-modified graphene; [Hmim][NTf_2]@LDHN-6: 1-hexyl-3-methylimidazolium bis(trifluoromethylsulfonyl)imide@liquid-decorated layered double hydroxide nanocage; IL: ionic liquids; KAUST-7: Ni(II)-pyrazine square-grid layers with $(NbOF5)^{2-}$ pillars; MCM-41: mobil composition of matter No. 41; MFI-ns: mordenite framework inverted nanosheets; MIL-53: matériaux de l'Institut Lavoisier n°53 ($Al(OH)[O_2C–C_6H_4–CO_2]\cdot[O_2C–C_6H_4–CO_2]0.7$); MIL-101: matériaux de l'Institut Lavoisier n°101; MIL-53(Al): aluminum-based MIL-53; MIL-101(Cr): chromium-based MIL-101; MOF: metal organic framework; MSS-Z8: meso–microporous silica-(ZIF-8) spheres; MWCNT: multi-walled carbon nanotube; NaY: Na^+ ion-exchanged zeolite; NH_2-MIL-53(Al): amine-functionalized aluminum metal-organic framework; NH_2-MIL-125(Ti): amine-functionalized titanium metal-organic framework; Ni-ns: nickel nanosheets; PDA-Ag^+: polydopamine (PDA) sphere and silver species; Pebax: poly(ether-block-amide); PEI: polyetherimide; PEO: polyethylene oxide; PIM: Polymer of intrinsic microporosity; PMPS: polymethylphenylsiloxane; PNT@NiCo-LDH: NiCo-layered double hydroxide-decorated polypyrrole nanotubes; POSS: polyhedral oligomeric silsesquioxane; PSf-Ac: polysulfone-acrylate; PU: polyurethane; SAPO: silico-alumino phosphate; S-MIL-101(Cr): sulfonated metal organic framework; Sm-NaY zeolite SNW-1: Schiff base network; Sm: silane-modified zeolite; SO_3H-MCM-41: sulfonic acid-functionalized MCM-41; SPEEK: sulfonated poly ether ether ketone; T: T-type zeolite; TA: tannic acid; TEPA-TiNTs: tetraethylene pentamine functionalized titanium oxide nanotubes; TiO_2–DA–PEI: amine-functionalized titania submicrospheres; TNT-IM: aminated titania nanotubes; TS-1: titanium silicate 1; UiO-66: Universitetet i Oslo [$Zr_6O_4(OH)_4(O_2CC_6H_4CO_2)_6$]; UiO-66-NH-$COCH_3$: amino-functionalized UiO-66 to acetamide; ZIF-8/ambz: zeolitic imidazolate framework-8/2-aminobenzimidazole; ZIF-67/RTIL: zeolitic imidazolate framework-67/Room temperature ionic liquid; $ZnCo_2O_4$: zinc cobaltate nanosheets; ZSM-5: zeolite socony mobil – 5; 6FDA: 4, 4′-(Hexafluoroisopropylidene) diphthalic anhydride.

Table 5
Comparison of upgrading technologies in term of costs and energy demands [23,191–194].

		Membrane separation	Water scrubbing	Chemical scrubbing	Organic scrubbing	PSA	Photosynthetic
Investment costs (€ $(Nm^3\ h^{-1})^{-1}$)	$<250\ Nm^3\ h^{-1}$	4700–6000	4000–5000	4500–5000	4000–5000	4500–5400	-
	$250–500\ Nm^3\ h^{-1}$	2700–4700	2500–4000	3000–4500	3000–4000	2500–4500	6000 (300 $Nm^3\ h^{-1}$)
	$5000–1000\ Nm^3\ h^{-1}$	1300–2700	1000–2500	2000–3000	1000–3000	1750–2500	-
Operating costs (€ Nm^{-3})		0.2	0.13	0.40	-	0.18	0.03
Energy demands (kWh Nm^{-3})		0.2–0.38	0.25–0.3	0.67–0.7	0.4–0.51	0.24–0.6	0.08–0.14

initial investment costs) are reasonable for long-term operation [23]. Otherwise, operating costs typically include membrane replacement (every 5–10 years), pressurizing biogas before separation and biogas pre-treatment costs.

Multiple challenges must be overcome to reduce operating and capital costs, thereby positioning membranes as the benchmark technology for small-, medium-, and large-scale biogas/biomethane production plants. Overall, conventional polymeric membranes support low CO_2 permeability or low selectivity in the separation of CO_2/CH_4, thus requiring two or more membrane modules to ensure high purity of the resulting CH_4 and CO_2 streams. Another critical drawback of conventional polymeric membranes is their low mechanical resistance under high pressure conditions and their tendency to plasticize with high CO_2 concentrations. On the other hand, the poor manufacturing reproducibility and high production costs of inorganic membranes, specifically zeolite-based membranes (2000–3000 € m^{-2}) remain as the critical drawbacks to tackle towards the widespread application of this material in small- and medium-size biogas production plants. Thinner membranes would result in lower diffusion resistance, higher efficiency, and reduced membrane costs, but current methods produce membranes 2–10 μm thick [98]. Reducing zeolite membrane thickness to ~100 nm, similar to polymer membranes, is highly desirable but very challenging. Therefore, most efforts are focused on developing new methods for synthesizing ultrathin zeolite-based membranes. MMM, which combines the advantages of polymeric and inorganic membranes, have also emerged as the next-generation materials for biogas separation. The main challenges to overcome of MMM include the fabrication of defect-free membranes with a high selectivity in the separation of CO_2/CH_4, which maintains a high mechanical/thermal resistance in the long-term operation. Research efforts are mainly concentrated in the development MMM targeting biogas separation. In addition, recent advances in membrane-based biogas upgrading focus on the development of improved process configuration. A single-stage configuration is not used because it is limited by high CH_4 losses and requires a higher energy cost for compression. Although two- and three-stage systems are common, multi-stage configurations are being explored to reduce costs and increase CH_4 purity and biomethane recovery [53].

H_2S, VMS and NH_3 are among the most important biogas pollutants, being also detrimental gases for several types of polymeric membranes. When biogas is separated by means of membrane technologies, a previous H_2S and NH_3 purification step is typically required to avoid membrane deterioration. Nowadays, many membranes have been developed for the separation of CO_2/CH_4, but few studies have considered the development of membranes for simultaneous separation of CO_2 and H_2S [123,124,197–199]. Although polymers with polar groups like ether linkages, pristine or modified MOFs and their MMMs, are expected to exhibit a good H_2S separation performance due to their high H_2S/CH_4 selectivity, experimental evidence of H_2S separation and membrane durability in the presence of H_2S are scarce in the literature [142,200]. UiO-66 MOFs were systematically evaluated for their effectiveness in removing NH_3 during air purification processes [201]. However, no studies have been conducted specifically with biogas. In addition, only a limited number of studies have recently investigated siloxane adsorption in membranes using hydrophobic MOFs, such as MIL-101 and Zr-MOF PCN-777, and these have focused exclusively on siloxane D4 (octamethylcyclotetrasiloxane) [202,203].

Future research should prioritize the enhancement of membrane materials to overcome the aforementioned challenges. In particular, exploring the development of FT-MMMs through the incorporation of ILs and amine-functionalized materials could be valuable for industrial applications. Furthermore, separation performance of biogas laden with common biogas pollutants, such as H_2S, NH_3 and VMS remain as a critical research niche that deserve further investigation. Finally, performance evaluation under long-term operation (i.e. weeks or months) and in wet conditions has become a crucial research focus for membranes intended for biogas separation.

5. Conclusions

Studies performed at lab and full-scale conditions have demonstrated that membranes constitute a technology platform capable of upgrading biogas into biomethane (CH_4 concentration > 90–95 % v v^{-1}) and CO_2 streams, which can be further valorized. New developments on polymeric membranes showed that FT membranes are currently the only type of polymeric membranes capable of achieving high CO_2 permeability at low feed pressures, while polymeric membranes based on 6FDA are the only ones with the potential to separate simultaneously H_2S and CO_2. If the best performing membrane for biogas separation must achieve the highest selectivity and permeability at the lowest operating pressure, then next-generation membranes can be ranked as follows based on their performance reported in the literature: FT-MMM > MOF-MMM > Zeolite-MMM. However, it must be stressed that even when FT-MMM are apparently the most promising membranes for CO_2/CH_4 separation, no data on CH_4 concentration in the retentate or stage cut values have been reported for these membranes. Such missing information is necessary to assess adequately the potential of these membranes and make fair comparisons with other types of MMM.

CRediT authorship contribution statement

Guillermo Quijano: Writing – review & editing, Writing – original draft, Visualization, Conceptualization. **Armando González-Sánchez:** Writing – review & editing. **Héctor A. Ruiz:** Writing – review & editing. **Raúl Muñoz:** Writing – review & editing. **Maria Del Rosario Rodero:** Writing – original draft.

Declaration of Competing Interest

The authors declare that they have no known competing financial interests or personal relationships that could have appeared to influence the work reported in this paper.

Data availability

No data was used for the research described in the article.

Acknowledgements

M. del R. Rodero acknowledges the NextGenerationEU Margarita Salas programme from the European Union for her research contract.

The Regional Government of Castilla y León and the EU-FEDER Program [grant number CL-EI-2021-07 and UIC 315] are also gratefully acknowledged.

References

[1] International Energy Agency, IEA World Energy Balances, 2021.

[2] IPCC, Climate Change 2022: Impacts, Adaptation and Vulnerability., UK and New York, NY, USA., 2022.

[3] Z. Jiang, A. Rahman Mahmud, A. Maneengam, A.A. Nassani, M. Haffar, P. The Cong,, Non linear effect of Biomass, fossil fuels and renewable energy usage on the economic growth: managing sustainable development through energy sector, Fuel 326 (2022) 124943, https://doi.org/10.1016/j.fuel.2022.124943.

[4] S. Spitzer, M. Miltner, M. Harasek, Investigation on the influence of membrane selectivity on the performance of mobile biogas upgrading plants by process simulation, J. Clean. Prod. 231 (2019) 43–53, https://doi.org/10.1016/j.jclepro.2019.05.105.

[5] I. Yasmeen, A. Ilyas, Z. Shamair, M.A. Gilani, S. Rafiq, M.R. Bilad, A.L. Khan, Synergistic effects of highly selective ionic liquid confined in nanocages: exploiting the three component mixed matrix membranes for CO2 capture, Chem. Eng. Res. Des. 155 (2020) 123–132, https://doi.org/10.1016/j.cherd.2020.01.006.

[6] Y.-G. Lim, C. Bak, Y.-D. Kim, Comprehensive experimental and theoretical insights into the performance of polysulfone hollow-fiber membrane modules in biogas purification process, Chem. Eng. J. 433 (2022) 134616, https://doi.org/10.1016/j.cej.2022.134616.

[7] N. Fajrina, N. Yusof, A.F. Ismail, F. Aziz, M.R. Bilad, M. Alkahtani, A crucial review on the challenges and recent gas membrane development for biogas upgrading, J. Environ. Chem. Eng. 11 (2023) 110235, https://doi.org/10.1016/j.jece.2023.110235.

[8] P. Gkotsis, P. Kougias, M. Mitrakas, A. Zouboulis, Biogas upgrading technologies – recent advances in membrane-based processes, Int. J. Hydrog. Energy 48 (2023) 3965–3993, https://doi.org/10.1016/j.ijhydene.2022.10.228.

[9] M.S. Shin, K.-H. Jung, J.-H. Kwag, Y.-W. Jeon, Biogas separation using a membrane gas separator: focus on CO2 upgrading without CH4 loss, Process Saf. Environ. Prot. 129 (2019) 348–358, https://doi.org/10.1016/j.psep.2019.07.020.

[10] D.Ó. Céileachair, R. O'Shea, J.D. Murphy, D.M. Wall, A methodology for designing biogas pipelines, Fuel 361 (2024) 130633, https://doi.org/10.1016/j.fuel.2023.130633.

[11] I. Moreno-Andrade, G. Moreno, G. Quijano, Theoretical framework for the estimation of H2S concentration in biogas produced from complex sulfur-rich substrates, Environ. Sci. Pollut. Res. 27 (2020) 15959–15966, https://doi.org/10.1007/s11356-019-04846-3.

[12] L. Rivera-Montenegro, E.I. Valenzuela, A. González-Sánchez, R. Muñoz, G. Quijano, Volatile methyl siloxanes as key biogas pollutants: occurrence, impacts and treatment technologies, BioEnergy Res 16 (2023) 801–816, https://doi.org/10.1007/s12155-022-10525-y.

[13] M. del Rosario Rodero, R. Ángeles, O. García-Depraect, R. Lebrero, R. Muñoz, Chapter 5 - Recent advances on photosynthetic biogas upgrading to biomethane, in: A. Yousuf, L. Melville (Eds.), Biogas to Biomethane, Woodhead Publishing, 2024, pp. 117–140, https://doi.org/10.1016/B978-0-443-18479-6.00010-7.

[14] P. San-Valero, J.M. Penya-roja, F. Javier Álvarez-Hornos, G. Buitrón, C. Gabaldón, G. Quijano, Fully aerobic bioscrubber for the desulfurization of H2S-rich biogas, Fuel 241 (2019) 884–891, https://doi.org/10.1016/j.fuel.2018.12.098.

[15] M. del R. Rodero, C.A. Severi, R. Rocher-Rivas, G. Quijano, R. Muñoz, Long-term influence of high alkalinity on the performance of photosynthetic biogas upgrading, Fuel 281 (2020) 118804, https://doi.org/10.1016/j.fuel.2020.118804.

[16] M. del R. Rodero, R. Ángeles, D. Marín, I. Díaz, A. Colzi, E. Posadas, R. Lebrero, R. Muñoz, Biogas purification and upgrading technologies, in: Biogas Fundam. Process. Oper, Springer, 2018, https://doi.org/10.1007/978-3-319-77335-3.

[17] R. Kapoor, P. Ghosh, M. Kumar, V.K. Vijay, Evaluation of biogas upgrading technologies and future perspectives: a review, Environ. Sci. Pollut. Res. 26 (2019) 11631–11661, https://doi.org/10.1007/s11356-019-04767-1.

[18] S. Mares, I. Moreno-Andrade, G. Quijano, Biological CH4 production from H2/CO2 streams: influence of trace metals concentration on the hydrogenotrophic process, J. Environ. Chem. Eng. 11 (2023) 109528, https://doi.org/10.1016/j.jece.2023.109528.

[19] C. Pascual, S. Cantera, R. Muñoz, R. Lebrero, Siloxanes removal in a two-phase partitioning biotrickling filter: influence of the EBRT and the organic phase, Renew. Energy 177 (2021) 52–60, https://doi.org/10.1016/j.renene.2021.05.144.

[20] R. Rocher-Rivas, A. González-Sánchez, G. Ulloa-Mercado, R. Muñoz, G. Quijano, Biogas desulfurization and calorific value enhancement in compact H2S/CO2 absorption units coupled to a photobioreactor, J. Environ. Chem. Eng. 10 (2022) 108336, https://doi.org/10.1016/j.jece.2022.108336.

[21] P.S. Goh, A.F. Ismail, - Introduction, in: P.S. Goh, A.F. Ismail (Eds.), Nanocomposite Membr. Gas Sep, Elsevier, 2020, pp. 1–19, https://doi.org/10.1016/B978-0-12-819406-5.00001-0.

[22] A.M. Yousef, W.M. El-Maghlany, Y.A. Eldrainy, A. Attia, Upgrading biogas to biomethane and liquid CO2: a novel cryogenic process, Fuel 251 (2019) 611–628, https://doi.org/10.1016/j.fuel.2019.03.127.

[23] R. Muñoz, L. Meier, I. Diaz, D. Jeison, A review on the state-of-the-art of physical/chemical and biological technologies for biogas upgrading, Rev. Environ. Sci. Biotechnol. 14 (2015) 727–759, https://doi.org/10.1007/s11157-015-9379-1.

[24] EBA, European Biogas Association. Statistical report 2022. Tracking biogas and biomethane deployment across Europe., Brussels, 2022.

[25] F. Kadirkhan, P.S. Goh, A.F. Ismail, W.N.F. Wan Mustapa, M.H.M. Halim, W. K. Soh, S.Y. Yeo, Recent advances of polymeric membranes in tackling plasticization and aging for practical industrial CO2/CH4 applications—a review, Membranes 12 (2022), https://doi.org/10.3390/membranes12010071.

[26] A. Roozitalab, F. Hamidavi, A. Kargari, A review of membrane material for biogas and natural gas upgrading, Gas. Sci. Eng. 114 (2023) 204969, https://doi.org/10.1016/j.jgsce.2023.204969.

[27] S.S. Hosseini, M. Azadi Tabar, I.F.J. Vankelecom, J.F.M. Denayer, Progress in high performance membrane materials and processes for biogas production, upgrading and conversion, Sep. Purif. Technol. 310 (2023) 123139, https://doi.org/10.1016/j.seppur.2023.123139.

[28] Y. Cheng, X. Wang, C. Jia, Y. Wang, L. Zhai, Q. Wang, D. Zhao, Ultrathin mixed matrix membranes containing two-dimensional metal-organic framework nanosheets for efficient CO2/CH4 separation, J. Membr. Sci. 539 (2017) 213–223, https://doi.org/10.1016/j.memsci.2017.06.011.

[29] P.F. Zito, A. Brunetti, G. Barbieri, 13 - Advanced membrane-based processes for biogas upgrading, in: A. Iulianelli, A. Cassano, C. Conidi, K. Petrotos (Eds.), Membr. Eng. Circ. Econ., Elsevier, 2022, pp. 345–373, https://doi.org/10.1016/B978-0-323-85253-1.00002-2.

[30] C. Soto, L. Palacio, R. Muñoz, P. Prádanos, A. Hernandez, Recent advances in membrane-based biogas and biohydrogen upgrading, Processes 10 (2022), https://doi.org/10.3390/pr10101918.

[31] IEA Bioenergy, A perspective on the state of the biogas industry from selected member countries of IEA Bioenergy Task 37, 2022. ⟨https://www.ieabioenergy.com/wp-content/uploads/2022/03/IEA_T37_CountryReportSummary_2021.pdf⟩.

[32] Y. Liu, J. Sim, R.H. Hailemariam, J. Lee, H. Rho, K.-D. Park, D.W. Kim, Y.C. Woo, Status and future trends of hollow fiber biogas separation membrane fabrication and modification techniques, Chemosphere 303 (2022) 134959, https://doi.org/10.1016/j.chemosphere.2022.134959.

[33] A.R. Teixeira Cardoso, A. Ambrosi, M. Di Luccio, D. Hotza, Membranes for separation of CO2/CH4 at harsh conditions, J. Nat. Gas Sci. Eng. 98 (2022) 104388, https://doi.org/10.1016/j.jngse.2021.104388.

[34] E. Nagy, 1 - On mass transport through a membrane layer, in: E. Nagy (Ed.), Basic Equations Mass Transp. through a Membr. Layer, Elsevier, Oxford, 2012, pp. 1–34, https://doi.org/10.1016/B978-0-12-416025-5.00001-6.

[35] B.K. Behera, R. Prasad, Chapter 2 - Greenhouse gas capture and conversion, in: B. K. Behera, R. Prasad (Eds.), Environ. Technol. Sustain., Elsevier, 2020, pp. 41–71, https://doi.org/10.1016/B978-0-12-819103-3.00002-0.

[36] Tadashi Uragami, Fundamentals of membrane transport phenomena, in: in: Sci. Technol. Sep. Membr., John Wiley & Sons, Ltd, 2017, pp. 147–180, https://doi.org/10.1002/9781118932551.ch6.

[37] S.S. Karim, T. Matsuura, A. Hussain, S. Farrukh, Facilitated transport membranes (ftms) gas transport models and reaction mechanism, in: S. Farrukh, X. Fan, T. Matsuura, S.S. Karim (Eds.), Facil. Transp. Membr. CO2 Capture Overv. Futur. Trends, Springer International Publishing, Cham, 2023, pp. 25–45, https://doi.org/10.1007/978-3-031-21444-8_2.

[38] H. Guo, J. Wei, Y. Ma, J. Deng, S. Yi, B. Wang, L. Deng, X. Jiang, Z. Dai, Facilitated transport membranes for CO2/CH4 separation - State of the art, Adv. Membr. 2 (2022) 100040, https://doi.org/10.1016/j.advmem.2022.100040.

[39] Y. Han, W.S.W. Ho, Recent advances in polymeric facilitated transport membranes for carbon dioxide separation and hydrogen purification, J. Polym. Sci. 58 (2020) 2435–2449, https://doi.org/10.1002/pol.20200187.

[40] M. Zhang, L. Chen, K. Wang, R. Lin, Z. Xiao, R. Semiat, X. He, Molecular engineering of copoly(ionic liquids)-based membranes for CO2 separation, ACS Appl. Polym. Mater. 6 (2024) 1853–1863, https://doi.org/10.1021/acsapm.3c02713.

[41] N. Jusoh, Y.F. Yeong, T.L. Chew, K.K. Lau, A.M. Shariff, Current development and challenges of mixed matrix membranes for CO2/CH4 separation, Sep. \ Purif. Rev. 45 (2016) 321–344. ⟨https://api.semanticscholar.org/CorpusID:100618686⟩.

[42] S. Sato, K. Nagai, Chapter 9 - Synthetic polymer-based membranes for acidic gas removal, in: A.F. Ismail, W.N.W. Salleh, N. Yusof (Eds.), Synth. Polym. Membr. Adv. Water Treat. Gas Sep. Energy Sustain., Elsevier, 2020, pp. 173–190, https://doi.org/10.1016/B978-0-12-818485-1.00009-5.

[43] E. Lasseuguette, M.-C. Ferrari, Chapter 10 - polymer membranes for sustainable gas separation, in: G. Szekely, A. Livingston (Eds.), Sustain. Nanoscale Eng., Elsevier, 2020, pp. 265–296, https://doi.org/10.1016/B978-0-12-814681-1.00010-2.

[44] L.G. Enrico Drioli, Encyclopedia of Membranes, Springer Berlin, Heidelberg, 2016, https://doi.org/10.1007/978-3-662-44324-8.

[45] A.F. Ismail, K.C. Khulbe, T. Matsuura, Fundamentals of gas permeation through membranes, in: in: Gas Sep. Membr. Polym. Inorg, Springer International Publishing, Cham, 2015, pp. 11–35, https://doi.org/10.1007/978-3-319-01095-3_2.

[46] D.R. Paul. Polymeric Gas Separation Membranes, first ed., CRC Press, 1994 https://doi.org/10.1201/9781351075886.

[47] T. Harlacher, M. Wessling, Chapter thirteen - gas–gas separation by membranes, in: S. Tarleton (Ed.), Prog. Filtr. Sep., Academic Press, Oxford, 2015, pp. 557–584, https://doi.org/10.1016/B978-0-12-384746-1.00013-6.

[48] G.G. Kagramanov, E.N. Farnosova, Scientific and engineering principles of membrane gas separation systems development, Theor. Found. Chem. Eng. 51 (2017) 38–44, https://doi.org/10.1134/S0040579517010092.

[49] S. Gilassi, S.M. Taghavi, D. Rodrigue, S. Kaliaguine, Optimizing membrane module for biogas separation, Int. J. Greenh. Gas Control. 83 (2019) 195–207, https://doi.org/10.1016/j.ijggc.2019.02.010.

[50] J.R. Rivero, L.R. Nemetz, M.M. Da Conceicao, G. Lipscomb, K. Hornbostel, Modeling gas separation in flat sheet membrane modules: impact of flow channel size variation, Carbon Capture Sci. Technol. 6 (2023) 100093, https://doi.org/10.1016/j.ccst.2022.100093.

[51] B. Castro-Dominguez, P. Leelachaikul, S.B. Messaoud, A. Takagaki, T. Sugawara, R. Kikuchi, S.T. Oyama, The optimal point within the Robeson upper boundary, Chem. Eng. Res. Des. 97 (2015) 109–119, https://doi.org/10.1016/j.cherd.2015.03.002.

[52] M. Purkait, R. Singh. Membrane Technology in Separation Science, first ed., CRC Press, 2018 https://doi.org/10.1201/9781315229263.

[53] F.M. Baena-Moreno, E. le Saché, L. Pastor-Pérez, T.R. Reina, Membrane-based technologies for biogas upgrading: a review, Environ. Chem. Lett. 18 (2020) 1649–1658, https://doi.org/10.1007/s10311-020-01036-3.

[54] B. Gye, I. Kammakakam, H. You, S. Nam, T.-H. Kim, PEG-imidazolium-incorporated polyimides as high-performance CO2-selective polymer membranes: the effects of PEG-imidazolium content, Sep. Purif. Technol. 179 (2017) 283–290, https://doi.org/10.1016/j.seppur.2017.02.020.

[55] X. Li, Y. Wang, T. Wu, S. Song, B. Wang, S. Zhong, R. Zhou, High-performance SSZ-13 membranes prepared using ball-milled nanosized seeds for carbon dioxide and nitrogen separations from methane, Chin. J. Chem. Eng. 28 (2020) 1285–1292, https://doi.org/10.1016/j.cjche.2020.02.004.

[56] M. Scholz, T. Melin, M. Wessling, Transforming biogas into biomethane using membrane technology, Renew. Sustain. Energy Rev. 17 (2013) 199–212, https://doi.org/10.1016/j.rser.2012.08.009.

[57] C. Koutsiantzi, M. Mitrakas, A. Zouboulis, I. Kellartzis, G. Stavropoulos, E. S. Kikkinides, Evaluation of polymeric membranes' performance during laboratory-scale experiments, regarding the CO2 separation from CH4, Chemosphere 299 (2022) 134224, https://doi.org/10.1016/j.chemosphere.2022.134224.

[58] M.S. Seong, C.I. Kong, B.R. Park, Y. Lee, B.K. Na, J.H. Kim, Optimization of pilot-scale 3-stage membrane process using asymmetric polysulfone hollow fiber membranes for production of high-purity CH4 and CO2 from crude biogas, Chem. Eng. J. 384 (2020) 123342, https://doi.org/10.1016/j.cej.2019.123342.

[59] N. Nemestóthy, P. Bakonyi, E. Szentgyörgyi, G. Kumar, D.D. Nguyen, S.W. Chang, S.-H. Kim, K. Bélafi-Bakó, Evaluation of a membrane permeation system for biogas upgrading using model and real gaseous mixtures: the effect of operating conditions on separation behaviour, methane recovery and process stability, J. Clean. Prod. 185 (2018) 44–51, https://doi.org/10.1016/j.jclepro.2018.03.047.

[60] J. Peppers, Y. Li, J. Xue, X. Chen, C. Alaimo, L. Wong, T. Young, P.G. Green, B. Jenkins, R. Zhang, M.J. Kleeman, Performance analysis of membrane separation for upgrading biogas to biomethane at small scale production sites, Biomass Bioenergy 128 (2019) 105314, https://doi.org/10.1016/j.biombioe.2019.105314.

[61] A.G. Chmielewski, A. Urbaniak, K. Wawryniuk, Membrane enrichment of biogas from two-stage pilot plant using agricultural waste as a substrate, Biomass Bioenergy 58 (2013) 219–228, https://doi.org/10.1016/j.biombioe.2013.08.010.

[62] M. Žák, H. Bendová, K. Friess, J.E. Bara, P. Izák, Single-step purification of raw biogas to biomethane quality by hollow fiber membranes without any pretreatment – An innovation in biogas upgrading, Sep. Purif. Technol. 203 (2018) 36–40, https://doi.org/10.1016/j.seppur.2018.04.024.

[63] A. Molino, F. Nanna, M. Migliori, P. Iovane, Y. Ding, B. Bikson, Experimental and simulation results for biomethane production using peek hollow fiber membrane, Fuel 112 (2013) 489–493, https://doi.org/10.1016/j.fuel.2013.04.046.

[64] P. Iovane, F. Nanna, Y. Ding, B. Bikson, A. Molino, Experimental test with polymeric membrane for the biogas purification from CO$_2$ and H$_2$S, Fuel 135 (2014) 352–358, https://doi.org/10.1016/j.fuel.2014.06.060.

[65] P. Dolejš, V. Poštulka, Z. Sedláková, V. Jandová, J. Vejražka, E. Esposito, J. C. Jansen, P. Izák, Simultaneous hydrogen sulphide and carbon dioxide removal from biogas by water–swollen reverse osmosis membrane, Sep. Purif. Technol. 131 (2014) 108–116, https://doi.org/10.1016/j.seppur.2014.04.041.

[66] M. Simcik, M.C. Ruzicka, M. Karaszova, Z. Sedlakova, J. Vejrazka, M. Vesely, P. Capek, K. Friess, P. Izak, Polyamide thin-film composite membranes for potential raw biogas purification: experiments and modeling, Sep. Purif. Technol. 167 (2016) 163–173, https://doi.org/10.1016/j.seppur.2016.05.008.

[67] P.D. Sutrisna, J. Hou, H. Li, Y. Zhang, V. Chen, Improved operational stability of Pebax-based gas separation membranes with ZIF-8: A comparative study of flat sheet and composite hollow fibre membranes, J. Membr. Sci. 524 (2017) 266–279, https://doi.org/10.1016/j.memsci.2016.11.048.

[68] M.E. Kojabad, A. Babaluo, A. Tavakoli, A novel semi-mobile carrier facilitated transport membrane containing aniline/poly (ether-block-amide) for CO2/N2 separation: molecular simulation and experimental study, Sep. Purif. Technol. 266 (2021) 118494, https://doi.org/10.1016/j.seppur.2021.118494.

[69] M.A. Llosa Tanco, J.A. Medrano, F. Gallucci, D.A. Pacheco Tanaka, Chapter 17 - membrane optimization and process condition investigation for enhancing the co2 separation from natural gas, in: A. Basile, E.P. Favvas (Eds.), Curr. Trends Futur. Dev. Membr, Elsevier, 2018, pp. 469–509, https://doi.org/10.1016/B978-0-12-813645-4.00017-9.

[70] M. Scholz, M. Alders, T. Lohaus, M. Wessling, Structural optimization of membrane-based biogas upgrading processes, J. Membr. Sci. 474 (2015) 1–10, https://doi.org/10.1016/j.memsci.2014.08.032.

[71] N. Alaslai, B. Ghanem, F. Alghunaimi, E. Litwiller, I. Pinnau, Pure- and mixed-gas permeation properties of highly selective and plasticization resistant hydroxyl-diamine-based 6FDA polyimides for CO2/CH4 separation, J. Membr. Sci. 505 (2016) 100–107, https://doi.org/10.1016/j.memsci.2015.12.053.

[72] J.A. Medrano, M.A. Llosa-Tanco, D.A. Pacheco Tanaka, F. Gallucci, Membranes utilization for biogas upgrading to synthetic natural gas, in: M. Materazzi, P. U. Foscolo (Eds.), Substit. Nat. Gas from Waste, 10, Academic Press, 2019, pp. 245–274, https://doi.org/10.1016/B978-0-12-815554-7.00010-6.

[73] L. Lei, A. Lindbråthen, X. Zhang, E.P. Favvas, M. Sandru, M. Hillestad, X. He, Preparation of carbon molecular sieve membranes with remarkable CO2/CH4 selectivity for high-pressure natural gas sweetening, J. Membr. Sci. 614 (2020) 118529, https://doi.org/10.1016/j.memsci.2020.118529.

[74] P. Du, X. Liang, L. You, X. Wang, J. Zhang, X. Ying, Z. Hong, Y. Zhang, X. Gu, Fabrication of high-selective hollow fiber DD3R zeolite membrane modules for high-pressure CO2/CH4 separation, J. Membr. Sci. 679 (2023) 121703, https://doi.org/10.1016/j.memsci.2023.121703.

[75] D. Meng, X. Kong, X. Tang, W. Guo, S. Yang, Y. Zhang, H. Qiu, Y. Zhang, Z. Zhang, Thin SAPO-34 zeolite membranes prepared by ball-milled seeds, Sep. Purif. Technol. 274 (2021) 118975, https://doi.org/10.1016/j.seppur.2021.118975.

[76] M. Wang, L. Bai, M. Li, L. Gao, M. Wang, P. Rao, Y. Zhang, Ultrafast synthesis of thin all-silica DDR zeolite membranes by microwave heating, J. Membr. Sci. 572 (2019) 567–579, https://doi.org/10.1016/j.memsci.2018.11.049.

[77] H. Verweij, Inorganic membranes, Curr. Opin. Chem. Eng. 1 (2012) 156–162, https://doi.org/10.1016/j.coche.2012.03.006.

[78] E. Yahya, G.P. Sean, A.F. Ismail, 5 - Membrane engineering in gas separation, in: A. Iulianelli, A. Cassano, C. Conidi, K. Petrotos (Eds.), Membr. Eng. Circ. Econ., Elsevier, 2022, pp. 123–147, https://doi.org/10.1016/B978-0-323-85253-1.00010-1.

[79] S. Farrukh, S. Ali, S.S. Karim, H. Waheed, I. Douna, Introduction, in: S. Farrukh, X. Fan, T. Matsuura, S.S. Karim (Eds.), Facil. Transp. Membr. CO2 Capture Overv. Futur. Trends, Springer International Publishing, Cham, 2023, pp. 1–24, https://doi.org/10.1007/978-3-031-21444-8_1.

[80] M. Kanezashi, T. Sasaki, H. Tawarayama, H. Nagasawa, T. Yoshioka, K. Ito, T. Tsuru, Experimental and theoretical study on small gas permeation properties through amorphous silica membranes fabricated at different temperatures, J. Phys. Chem. C 118 (2014) 20323–20331, https://doi.org/10.1021/jp504937t.

[81] M. Chen, W. Guo, X. Kong, X. Tang, S. Yang, D. Meng, L. Zhou, J. Ma, X. Du, Y. Zhang, Efficient and facile preparation of pure silica CHA zeolite membranes by gel-less method, J. Membr. Sci. 666 (2023) 121160, https://doi.org/10.1016/j.memsci.2022.121160.

[82] S. Basu, A.L. Khan, A. Cano-Odena, C. Liu, I.F.J. Vankelecom, Membrane-based technologies for biogas separations, Chem. Soc. Rev. 39 (2010) 750–768, https://doi.org/10.1039/B817050A.

[83] J. Okazaki, H. Hasegawa, N. Chikamatsu, K. Yajima, K. Shimizu, M. Niino, DDR-type zeolite membrane: a novel CO2 separation technology for enhanced oil recovery, Sep. Purif. Technol. 218 (2019) 200–205, https://doi.org/10.1016/j.seppur.2019.02.049.

[84] S. Araki, R. Yamashita, K. Li, H. Yamamoto, Preparation and gas permeation properties of all-silica CHA zeolite hollow fiber membranes prepared on amorphous-silica hollow fibers, J. Membr. Sci. 634 (2021) 119338, https://doi.org/10.1016/j.memsci.2021.119338.

[85] H. Liu, X. Gao, S. Wang, Z. Hong, X. Wang, X. Gu, SSZ-13 zeolite membranes on four-channel α-Al2O3 hollow fibers for CO2 separation, Sep. Purif. Technol. 267 (2021) 118611, https://doi.org/10.1016/j.seppur.2021.118611.

[86] X. Tang, Y. Zhang, D. Meng, X. Kong, L. Kong, H. Qiu, N. Xu, W. Guo, S. Yang, Y. Zhang, Efficient synthesis of thin SSZ-13 membranes by gel-less method, J. Membr. Sci. 620 (2021) 118920, https://doi.org/10.1016/j.memsci.2020.118920.

[87] H.H. Funke, M.Z. Chen, A.N. Prakash, J.L. Falconer, R.D. Noble, Separating molecules by size in SAPO-34 membranes, J. Membr. Sci. 456 (2014) 185–191, https://doi.org/10.1016/j.memsci.2014.01.032.

[88] M. Li, J. Zhang, X. Liu, Y. Wang, C. Liu, D. Hu, G. Zeng, Y. Zhang, W. Wei, Y. Sun, Synthesis of high performance SAPO-34 zeolite membrane by a novel two-step hydrothermal synthesis + dry gel conversion method, Microporous Mesoporous Mater. 225 (2016) 261–271, https://doi.org/10.1016/j.micromeso.2015.11.056.

[89] H. Qiu, Y. Zhang, L. Kong, X. Kong, X. Tang, D. Meng, N. Xu, M. Wang, Y. Zhang, High performance SSZ-13 membranes prepared at low temperature, J. Membr. Sci. 603 (2020) 118023, https://doi.org/10.1016/j.memsci.2020.118023.

[90] N. Xu, D. Meng, X. Tang, X. Kong, L. Kong, Y. Zhang, H. Qiu, M. Wang, Y. Zhang, Fast synthesis of thin all-silica DDR zeolite membranes with inorganic base as mineralizing agent for CO2-CH4 separation, Sep. Purif. Technol. 253 (2020) 117505, https://doi.org/10.1016/j.seppur.2020.117505.

[91] X. Tang, Y. Zhang, D. Meng, X. Kong, S. Yang, W. Guo, H. Qiu, L. Kong, Y. Zhang, Z. Zhang, Fast synthesis of thin SSZ-13 membranes by a hot-dipping method, J. Membr. Sci. 629 (2021) 119297, https://doi.org/10.1016/j.memsci.2021.119297.

[92] E. Hayakawa, S. Himeno, Synthesis of all-silica ZSM-58 zeolite membranes for separation of CO2/CH4 and CO2/N2 gas mixtures, Microporous Mesoporous Mater. 291 (2020) 109695, https://doi.org/10.1016/j.micromeso.2019.109695.

[93] W. Rahmah, G.T.M. Kadja, M.H. Mahyuddin, A.G. Saputro, H.K. Dipojono, I. G. Wenten, Small-pore zeolite and zeotype membranes for CO2 capture and sequestration – a review, J. Environ. Chem. Eng. 10 (2022) 108707, https://doi.org/10.1016/j.jece.2022.108707.

[94] S. Zhong, N. Bu, R. Zhou, W. Jin, M. Yu, S. Li, Aluminophosphate-17 and silicoaluminophosphate-17 membranes for CO2 separations, J. Membr. Sci. 520 (2016) 507–514, https://doi.org/10.1016/j.memsci.2016.08.010.

[95] W. Liu, Y. Tu, J. Lu, Y. Liu, T. Wu, T. Gui, X. Chen, H. Kita, AlPO-18 membranes for CO2/CH4 and N2/CH4 separations, Microporous Mesoporous Mater. 348 (2023) 112416, https://doi.org/10.1016/j.micromeso.2022.112416.

[96] L. Yu, S. Fouladvand, M. Grahn, J. Hedlund, Ultra-thin MFI membranes with different Si/Al ratios for CO2/CH4 separation, Microporous Mesoporous Mater. 284 (2019) 258–264, https://doi.org/10.1016/j.micromeso.2019.04.042.

[97] B. Wang, C. Sun, R. Zhou, W. Xing, A super-permeable and highly-oriented SAPO-34 thin membrane prepared by a green gel-less method using high-aspect-ratio nanosheets for efficient CO2 capture, Chem. Eng. J. 442 (2022) 136336, https://doi.org/10.1016/j.cej.2022.136336.

[98] Y. Zhang, M. Wang, H. Qiu, L. Kong, N. Xu, X. Tang, D. Meng, X. Kong, Y. Zhang, Synthesis of thin SAPO-34 zeolite membranes in concentrated gel, J. Membr. Sci. 612 (2020) 118451, https://doi.org/10.1016/j.memsci.2020.118451.

[99] Y. Chen, Y. Zhang, C. Zhang, J. Jiang, X. Gu, Fabrication of high-flux SAPO-34 membrane on α-Al2O3 four-channel hollow fibers for CO2 capture from CH4, J. CO2 Util. 18 (2017) 30–40, https://doi.org/10.1016/j.jcou.2017.01.005.

[100] J. Zhou, S. Wu, B. Liu, R. Zhou, W. Xing, Scalable fabrication of highly selective SSZ-13 membranes on 19-channel monolithic supports for efficient CO2 capture, Sep. Purif. Technol. 293 (2022) 121122, https://doi.org/10.1016/j.seppur.2022.121122.

[101] M. Lee, Y. Jeong, S. Hong, J. Choi, High performance CO2-perm-selective SSZ-13 membranes: elucidation of the link between membrane material and module properties, J. Membr. Sci. 611 (2020) 118390, https://doi.org/10.1016/j.memsci.2020.118390.

[102] B. Wang, Y. Zheng, J. Zhang, W. Zhang, F. Zhang, W. Xing, R. Zhou, Separation of light gas mixtures using zeolite SSZ-13 membranes, Microporous Mesoporous Mater. 275 (2019) 191–199, https://doi.org/10.1016/j.micromeso.2018.08.032.

[103] J. Kim, E. Jang, S. Hong, D. Kim, E. Kim, H. Ricther, A. Simon, N. Choi, D. Korelskiy, S. Fouladvand, J. Nam, J. Choi, Microstructural control of a SSZ-13 zeolite film via rapid thermal processing, J. Membr. Sci. 591 (2019) 117342, https://doi.org/10.1016/j.memsci.2019.117342.

[104] Y. Zheng, N. Hu, H. Wang, N. Bu, F. Zhang, R. Zhou, Preparation of steam-stable high-silica CHA (SSZ-13) membranes for CO2/CH4 and C2H4/C2H6 separation, J. Membr. Sci. 475 (2015) 303–310, https://doi.org/10.1016/j.memsci.2014.10.048.

[105] K. Kida, Y. Maeta, K. Yogo, Pure silica CHA-type zeolite membranes for dry and humidified CO2/CH4 mixtures separation, Sep. Purif. Technol. 197 (2018) 116–121, https://doi.org/10.1016/j.seppur.2017.12.060.

[106] X. Kong, H. Qiu, D. Meng, X. Tang, S. Yang, W. Guo, Y. Zhang, L. Kong, Y. Zhang, Z. Zhang, Reproducible synthesis of all-silica CHA zeolite membranes in a homogeneous mother liquor, Sep. Purif. Technol. 274 (2021) 119104, https://doi.org/10.1016/j.seppur.2021.119104.

[107] E. Jang, S. Hong, E. Kim, N. Choi, S.J. Cho, J. Choi, Organic template-free synthesis of high-quality CHA type zeolite membranes for carbon dioxide separation, J. Membr. Sci. 549 (2018) 46–59, https://doi.org/10.1016/j.memsci.2017.11.068.

[108] N.M. Nguyen, Q.T. Le, D.P.-H. Nguyen, T.N. Nguyen, T.T. Le, T.C.-T. Pham, Facile synthesis of seed crystals and gelless growth of pure silica DDR zeolite membrane on low cost silica support for high performance in CO2 separation, J. Membr. Sci. 624 (2021) 119110, https://doi.org/10.1016/j.memsci.2021.119110.

[109] L. Wang, C. Zhang, X. Gao, L. Peng, J. Jiang, X. Gu, Preparation of defect-free DDR zeolite membranes by eliminating template with ozone at low temperature, J. Membr. Sci. 539 (2017) 152–160, https://doi.org/10.1016/j.memsci.2017.06.004.

[110] S. Yang, Z. Cao, A. Arvanitis, X. Sun, Z. Xu, J. Dong, DDR-type zeolite membrane synthesis, modification and gas permeation studies, J. Membr. Sci. 505 (2016) 194–204, https://doi.org/10.1016/j.memsci.2016.01.043.

[111] T. Wu, B. Wang, Z. Lu, R. Zhou, X. Chen, Alumina-supported AlPO-18 membranes for CO2/CH4 separation, J. Membr. Sci. 471 (2014) 338–346, https://doi.org/10.1016/j.memsci.2014.08.035.

[112] L. Sandström, E. Sjöberg, J. Hedlund, Very high flux MFI membrane for CO2 separation, J. Membr. Sci. 380 (2011) 232–240, https://doi.org/10.1016/j.memsci.2011.07.011.

[113] M. Sen, K. Dana, N. Das, Development of LTA zeolite membrane from clay by sonication assisted method at room temperature for H2-CO2 and CO2-CH4 separation, Ultrason. Sonochem. 48 (2018) 299–310, https://doi.org/10.1016/j.ultsonch.2018.06.007.

[114] R. Swaidan, B. Ghanem, E. Litwiller, I. Pinnau, Effects of hydroxyl-functionalization and sub-Tg thermal annealing on high pressure pure- and mixed-gas CO2/CH4 separation by polyimide membranes based on 6FDA and triptycene-containing dianhydrides, J. Membr. Sci. 475 (2015) 571–581, https://doi.org/10.1016/j.memsci.2014.10.046.

[115] S. Fu, G.B. Wenz, E.S. Sanders, S.S. Kulkarni, W. Qiu, C. Ma, W.J. Koros, Effects of pyrolysis conditions on gas separation properties of 6FDA/DETDA:DABA(3:2) derived carbon molecular sieve membranes, J. Membr. Sci. 520 (2016) 699–711, https://doi.org/10.1016/j.memsci.2016.08.013.

[116] M.S. Nobandegani, L. Yu, J. Hedlund, Mass transport of CO2 over CH4 controlled by the selective surface barrier in ultra-thin CHA membranes, Microporous Mesoporous Mater. 332 (2022) 111716, https://doi.org/10.1016/j.micromeso.2022.111716.

[117] S. Mosleh, M.R. Mozdianfard, M. Hemmati, G. Khanbabaei, Synthesis and characterization of rubbery/glassy blend membranes for CO2/CH4 gas separation, J. Polym. Res. 23 (2016) 120, https://doi.org/10.1007/s10965-016-1005-6.

[118] H. Roafi, S. Farrukh, Z. Salahuddin, A. Raza, S.S. Karim, H. Waheed, Fabrication and permeation analysis of polysulfone (PSf) modified cellulose triacetate (CTA) blend membranes for CO2 separation from methane (CH4), J. Polym. Environ. 32 (2024) 2414–2430, https://doi.org/10.1007/s10924-023-03125-0.

[119] K. Maqsood, A. Jamil, A. Ahmed, B. Sutisna, S. Nunes, M. Ulbricht, Blend membranes comprising polyetherimide and polyvinyl acetate with improved methane enrichment performance, Chemosphere 321 (2023) 138074, https://doi.org/10.1016/j.chemosphere.2023.138074.

[120] A. Hayek, G.O. Yahaya, A. Alsamah, S.K. Panda, Fluorinated copolyimide membranes for sour mixed-gas upgrading, J. Appl. Polym. Sci. 137 (2020) 48336, https://doi.org/10.1002/app.48336.

[121] F. Alghunaimi, B. Ghanem, N. Alaslai, R. Swaidan, E. Litwiller, I. Pinnau, Gas permeation and physical aging properties of iptycene diamine-based microporous polyimides, J. Membr. Sci. 490 (2015) 321–327, https://doi.org/10.1016/j.memsci.2015.05.010.

[122] C. Ma, W.J. Koros, High-performance ester-crosslinked hollow fiber membranes for natural gas separations, J. Membr. Sci. 428 (2013) 251–259, https://doi.org/10.1016/j.memsci.2012.10.024.

[123] G.O. Yahaya, M.S. Qahtani, A.Y. Ammar, A.A. Bahamdan, A.W. Ameen, R. H. Alhajry, M.M.Ben Sultan, F. Hamad, Aromatic block co-polyimide membranes for sour gas feed separations, Chem. Eng. J. 304 (2016) 1020–1030, https://doi.org/10.1016/j.cej.2016.06.076.

[124] B. Kraftschik, W.J. Koros, J.R. Johnson, O. Karvan, Dense film polyimide membranes for aggressive sour gas feed separations, J. Memb. Sci. 428 (2013) 608–619, https://doi.org/10.1016/j.memsci.2012.10.025.

[125] H. Asghar, A. Ilyas, Z. Tahir, X. Li, A.L. Khan, Fluorinated and sulfonated poly (ether ether ketone) and Matrimid blend membranes for CO2 separation, Sep. Purif. Technol. 203 (2018) 233–241, https://doi.org/10.1016/j.seppur.2018.04.047.

[126] R. Swaidan, B.S. Ghanem, E. Litwiller, I. Pinnau, Pure- and mixed-gas CO2/CH4 separation properties of PIM-1 and an amidoxime-functionalized PIM-1, J. Membr. Sci. 457 (2014) 95–102, https://doi.org/10.1016/j.memsci.2014.01.055.

[127] R. Swaidan, X. Ma, E. Litwiller, I. Pinnau, High pressure pure- and mixed-gas separation of CO2/CH4 by thermally-rearranged and carbon molecular sieve membranes derived from a polyimide of intrinsic microporosity, J. Membr. Sci. 447 (2013) 387–394, https://doi.org/10.1016/j.memsci.2013.07.057.

[128] E. Ahmadpour, A.A. Shamsabadi, R.M. Behbahani, M. Aghajani, A. Kargari, Study of CO2 separation with PVC/Pebax composite membrane, J. Nat. Gas Sci. Eng. 21 (2014) 518–523, https://doi.org/10.1016/j.jngse.2014.09.021.

[129] X. Li, M. Wang, S. Wang, Y. Li, Z. Jiang, R. Guo, H. Wu, X. Cao, J. Yang, B. Wang, Constructing CO2 transport passageways in Matrimid® membranes using nanohydrogels for efficient carbon capture, J. Membr. Sci. 474 (2015) 156–166, https://doi.org/10.1016/j.memsci.2014.10.003.

[130] F. Emamverdi, J. Huang, N.M. Razavi, M.J. Bojdys, A.B. Foster, P.M. Budd, M. Böhning, A. Schönhals, Molecular mobility and gas transport properties of mixed matrix membranes based on PIM-1 and a phosphinine containing covalent organic framework, Macromolecules 57 (2024) 1829–1845, https://doi.org/10.1021/acs.macromol.3c02419.

[131] P.M. Budd, Chapter 9 - polymers of intrinsic microporosity and their potential in process intensification, in: G. Szekely, A. Livingston (Eds.), Sustain. Nanoscale Eng., Elsevier, 2020, pp. 231–264, https://doi.org/10.1016/B978-0-12-814681-1.00009-6.

[132] T. Alebrahim, L. Huang, H.K. Welgama, N. Esmaeili, E. Deng, S. Cheng, D. Acharya, C.M. Doherty, A.J. Hill, C. Rumsey, M. Trebbin, T.R. Cook, H. Lin, Low-loading mixed matrix materials: fractal-like structure and peculiarly enhanced gas permeability, ACS Appl. Mater. Interfaces 16 (2024) 11116–11124, https://doi.org/10.1021/acsami.3c19631.

[133] X. Wu, Z. Tian, S. Wang, D. Peng, L. Yang, Y. Wu, Q. Xin, H. Wu, Z. Jiang, Mixed matrix membranes comprising polymers of intrinsic microporosity and covalent organic framework for gas separation, J. Membr. Sci. 528 (2017) 273–283, https://doi.org/10.1016/j.memsci.2017.01.042.

[134] M. Barooah, S. Kundu, S. Kumar, A. Katare, R. Borgohain, R.V.S. Uppaluri, L. M. Kundu, B. Mandal, New generation mixed matrix membrane for CO2 separation: transition from binary to quaternary mixed matrix membrane, Chemosphere 354 (2024) 141653, https://doi.org/10.1016/j.chemosphere.2024.141653.

[135] M.Z. Ahmad, T.A. Peters, N.M. Konnertz, T. Visser, C. Téllez, J. Coronas, V. Fila, W.M. de Vos, N.E. Benes, High-pressure CO2/CH4 separation of Zr-MOFs based mixed matrix membranes, Sep. Purif. Technol. 230 (2020) 115858, https://doi.org/10.1016/j.seppur.2019.115858.

[136] S. Belhaj Messaoud, A. Takagaki, T. Sugawara, R. Kikuchi, S.T. Oyama, Mixed matrix membranes using SAPO-34/polyetherimide for carbon dioxide/methane separation, Sep. Purif. Technol. 148 (2015) 38–48, https://doi.org/10.1016/j.seppur.2015.04.017.

[137] M. Waqas Anjum, F. de Clippel, J. Didden, A. Laeeq Khan, S. Couck, G.V. Baron, J. F.M. Denayer, B.F. Sels, I.F.J. Vankelecom, Polyimide mixed matrix membranes for CO2 separations using carbon–silica nanocomposite fillers, J. Membr. Sci. 495 (2015) 121–129, https://doi.org/10.1016/j.memsci.2015.08.006.

[138] X. Chen, N. Wang, G. Chen, Z. Wang, G. Liu, R. Zhou, W. Jin, Zeolite/polyimide mixed-matrix membranes with enhanced natural gas purification performance: importance of filler structural integrity, J. Membr. Sci. 672 (2023) 121462, https://doi.org/10.1016/j.memsci.2023.121462.

[139] M.U.M. Junaidi, C.P. Leo, A.L. Ahmad, N.A. Ahmad, Fluorocarbon functionalized SAPO-34 zeolite incorporated in asymmetric mixed matrix membranes for carbon dioxide separation in wet gases, Microporous Mesoporous Mater. 206 (2015) 23–33, https://doi.org/10.1016/j.micromeso.2014.12.013.

[140] F. Dorosti, M. Omidkhah, R. Abedini, Enhanced CO2/CH4 separation properties of asymmetric mixed matrix membrane by incorporating nano-porous ZSM-5 and MIL-53 particles into Matrimid®5218, J. Nat. Gas Sci. Eng. 25 (2015) 88–102, https://doi.org/10.1016/j.jngse.2015.04.033.

[141] A. Ebadi Amooghin, M. Omidkhah, A. Kargari, The effects of aminosilane grafting on NaY zeolite–Matrimid®5218 mixed matrix membranes for CO2/CH4 separation, J. Membr. Sci. 490 (2015) 364–379, https://doi.org/10.1016/j.memsci.2015.04.070.

[142] Z. Duma, P.R. Makgwane, M. Masukume, A. Swartbooi, K. Rambau, T. Mehlo, T. Mavhungu, A comprehensive review of metal-organic frameworks sorbents and their mixed-matrix membranes composites for biogas cleaning and CO2/CH4 separation, Mater. Today Sustain. 27 (2024) 100812, https://doi.org/10.1016/j.mtsust.2024.100812.

[143] A.R. Kamble, C.M. Patel, Z.V.P. Murthy, A review on the recent advances in mixed matrix membranes for gas separation processes, Renew. Sustain. Energy Rev. 145 (2021) 111062, https://doi.org/10.1016/j.rser.2021.111062.

[144] A. Imtiaz, M.H.D. Othman, A. Jilani, I.U. Khan, R. Kamaludin, O. Samuel, ZIF-filler incorporated mixed matrix membranes (MMMs) for efficient gas separation: a review, J. Environ. Chem. Eng. 10 (2022) 108541, https://doi.org/10.1016/j.jece.2022.108541.

[145] M.Z. Ahmad, V. Martin-Gil, V. Perfilov, P. Sysel, V. Fila, Investigation of a new co-polyimide, 6FDA-bisP and its ZIF-8 mixed matrix membranes for CO2/CH4 separation, Sep. Purif. Technol. 207 (2018) 523–534, https://doi.org/10.1016/j.seppur.2018.06.067.

[146] M. Zamidi Ahmad, M. Navarro, M. Lhotka, B. Zornoza, C. Téllez, V. Fila, J. Coronas, Enhancement of CO2/CH4 separation performances of 6FDA-based co-polyimides mixed matrix membranes embedded with UiO-66 nanoparticles, Sep. Purif. Technol. 192 (2018) 465–474, https://doi.org/10.1016/j.seppur.2017.10.039.

[147] H. Gong, S.S. Lee, T.-H. Bae, Mixed-matrix membranes containing inorganically surface-modified 5A zeolite for enhanced CO2/CH4 separation, Microporous Mesoporous Mater. 237 (2017) 82–89, https://doi.org/10.1016/j.micromeso.2016.09.017.

[148] J. Zhao, K. Xie, L. Liu, M. Liu, W. Qiu, P.A. Webley, Enhancing plasticization-resistance of mixed-matrix membranes with exceptionally high CO2/CH4 selectivity through incorporating ZSM-25 zeolite, J. Membr. Sci. 583 (2019) 23–30, https://doi.org/10.1016/j.memsci.2019.03.073.

[149] N. Jusoh, Y.F. Yeong, K.K. Lau, A. M. Shariff, Enhanced gas separation performance using mixed matrix membranes containing zeolite T and 6FDA-durene polyimide, J. Membr. Sci. 525 (2017) 175–186, https://doi.org/10.1016/j.memsci.2016.10.044.

[150] N. Jusoh, Y.F. Yeong, K.K. Lau, A. M. Shariff, Fabrication of silanated zeolite T/6FDA-durene composite membranes for CO2/CH4 separation, J. Clean. Prod. 166 (2017) 1043–1058, https://doi.org/10.1016/j.jclepro.2017.08.080.

[151] S. Ishaq, R. Tamime, M.R. Bilad, A.L. Khan, Mixed matrix membranes comprising of polysulfone and microporous Bio-MOF-1: preparation and gas separation properties, Sep. Purif. Technol. 210 (2019) 442–451, https://doi.org/10.1016/j.seppur.2018.08.031.

[152] S. Shahid, K. Nijmeijer, Performance and plasticization behavior of polymer–MOF membranes for gas separation at elevated pressures, J. Membr. Sci. 470 (2014) 166–177, https://doi.org/10.1016/j.memsci.2014.07.034.

[153] F. Dorosti, A. Alizadehdakhel, Fabrication and investigation of PEBAX/Fe-BTC, a high permeable and CO2 selective mixed matrix membrane, Chem. Eng. Res. Des. 136 (2018) 119–128, https://doi.org/10.1016/j.cherd.2018.01.029.

[154] S. Shahid, K. Nijmeijer, High pressure gas separation performance of mixed-matrix polymer membranes containing mesoporous Fe(BTC), J. Membr. Sci. 459 (2014) 33–44, https://doi.org/10.1016/j.memsci.2014.02.009.

[155] K. Chen, K. Xu, L. Xiang, X. Dong, Y. Han, C. Wang, L.-B. Sun, Y. Pan, Enhanced CO2/CH4 separation performance of mixed-matrix membranes through dispersion of sorption-selective MOF nanocrystals, J. Membr. Sci. 563 (2018) 360–370, https://doi.org/10.1016/j.memsci.2018.06.007.

[156] N. Tien-Binh, H. Vinh-Thang, X.Y. Chen, D. Rodrigue, S. Kaliaguine, Crosslinked MOF-polymer to enhance gas separation of mixed matrix membranes, J. Membr. Sci. 520 (2016) 941–950, https://doi.org/10.1016/j.memsci.2016.08.045.

[157] S. Khoshhal Salestan, K. Pirzadeh, A. Rahimpour, R. Abedini, Poly (ether-block amide) thin-film membranes containing functionalized MIL-101 MOFs for efficient separation of CO2/CH4, J. Environ. Chem. Eng. 9 (2021) 105820, https://doi.org/10.1016/j.jece.2021.105820.

[158] S. Sorribas, B. Zornoza, C. Téllez, J. Coronas, Mixed matrix membranes comprising silica-(ZIF-8) core–shell spheres with ordered meso–microporosity for natural- and bio-gas upgrading, J. Membr. Sci. 452 (2014) 184–192, https://doi.org/10.1016/j.memsci.2013.10.043.

[159] S. Castarlenas, C. Téllez, J. Coronas, Gas separation with mixed matrix membranes obtained from MOF UiO-66-graphite oxide hybrids, J. Membr. Sci. 526 (2017) 205–211, https://doi.org/10.1016/j.memsci.2016.12.041.

[160] R. Castro-Muñoz, V. Fíla, V. Martin-Gil, C. Muller, Enhanced CO2 permeability in Matrimid® 5218 mixed matrix membranes for separating binary CO2/CH4 mixtures, Sep. Purif. Technol. 210 (2019) 553–562, https://doi.org/10.1016/j.seppur.2018.08.046.

[161] J.A. Thompson, J.T. Vaughn, N.A. Brunelli, W.J. Koros, C.W. Jones, S. Nair, Mixed-linker zeolitic imidazolate framework mixed-matrix membranes for aggressive CO2 separation from natural gas, Microporous Mesoporous Mater. 192 (2014) 43–51, https://doi.org/10.1016/j.micromeso.2013.06.036.

[162] N. Jusoh, Y.F. Yeong, W.L. Cheong, K.K. Lau, A. M. Shariff, Facile fabrication of mixed matrix membranes containing 6FDA-durene polyimide and ZIF-8 nanofillers for CO2 capture, J. Ind. Eng. Chem. 44 (2016) 164–173, https://doi.org/10.1016/j.jiec.2016.08.030.

[163] H.R. Amedi, M. Aghajani, Gas separation in mixed matrix membranes based on polyurethane containing SiO2, ZSM-5, and ZIF-8 nanoparticles, J. Nat. Gas Sci. Eng. 35 (2016) 695–702, https://doi.org/10.1016/j.jngse.2016.09.015.

[164] S. Shahid, K. Nijmeijer, S. Nehache, I. Vankelecom, A. Deratani, D. Quemener, MOF-mixed matrix membranes: precise dispersion of MOF particles with better compatibility via a particle fusion approach for enhanced gas separation properties, J. Membr. Sci. 492 (2015) 21–31, https://doi.org/10.1016/j.memsci.2015.05.015.

[165] L. Diestel, X.L. Liu, Y.S. Li, W.S. Yang, J. Caro, Comparative permeation studies on three supported membranes: pure ZIF-8, pure polymethylphenylsiloxane, and mixed matrix membranes, Microporous Mesoporous Mater. 189 (2014) 210–215, https://doi.org/10.1016/j.micromeso.2013.09.012.

[166] S. Meshkat, S. Kaliaguine, D. Rodrigue, Mixed matrix membranes based on amine and non-amine MIL-53(Al) in Pebax® MH-1657 for CO2 separation, Sep. Purif. Technol. 200 (2018) 177–190, https://doi.org/10.1016/j.seppur.2018.02.038.

[167] T. Rodenas, M. van Dalen, P. Serra-Crespo, F. Kapteijn, J. Gascon, Mixed matrix membranes based on NH2-functionalized MIL-type MOFs: influence of structural and operational parameters on the CO2/CH4 separation performance, Microporous Mesoporous Mater. 192 (2014) 35–42, https://doi.org/10.1016/j.micromeso.2013.08.049.

[168] X. Guo, H. Huang, Y. Ban, Q. Yang, Y. Xiao, Y. Li, W. Yang, C. Zhong, Mixed matrix membranes incorporated with amine-functionalized titanium-based metal-organic framework for CO2/CH4 separation, J. Membr. Sci. 478 (2015) 130–139, https://doi.org/10.1016/j.memsci.2015.01.007.

[169] M.R. Khdhayyer, E. Esposito, A. Fuoco, M. Monteleone, L. Giorno, J.C. Jansen, M. P. Attfield, P.M. Budd, Mixed matrix membranes based on UiO-66 MOFs in the polymer of intrinsic microporosity PIM-1, Sep. Purif. Technol. 173 (2017) 304–313, https://doi.org/10.1016/j.seppur.2016.09.036.

[170] M.Z. Ahmad, M. Navarro, M. Lhotka, B. Zornoza, C. Téllez, W.M. de Vos, N. E. Benes, N.M. Konnertz, T. Visser, R. Semino, G. Maurin, V. Fila, J. Coronas, Enhanced gas separation performance of 6FDA-DAM based mixed matrix membranes by incorporating MOF UiO-66 and its derivatives, J. Membr. Sci. 558 (2018) 64–77, https://doi.org/10.1016/j.memsci.2018.04.040.

[171] A.L. Khan, C. Klaysom, A. Gahlaut, A.U. Khan, I.F.J. Vankelecom, Mixed matrix membranes comprising of Matrimid and –SO3H functionalized mesoporous MCM-41 for gas separation, J. Membr. Sci. 447 (2013) 73–79, https://doi.org/10.1016/j.memsci.2013.07.011.

[172] Z. Gao, Y. Wang, H. Wu, Y. Ren, Z. Guo, X. Liang, Y. Wu, Y. Liu, Z. Jiang, Surface functionalization of Polymers of Intrinsic Microporosity (PIMs) membrane by polyphenol for efficient CO2 separation, Green Chem. Eng. 2 (2021) 70–76, https://doi.org/10.1016/j.gce.2020.12.003.

[173] X. Li, L. Ma, H. Zhang, S. Wang, Z. Jiang, R. Guo, H. Wu, X. Cao, J. Yang, B. Wang, Synergistic effect of combining carbon nanotubes and graphene oxide in mixed matrix membranes for efficient CO2 separation, J. Membr. Sci. 479 (2015) 1–10, https://doi.org/10.1016/j.memsci.2015.01.014.

[174] Y. Kinoshita, K. Wakimoto, A.H. Gibbons, A.P. Isfahani, H. Kusuda, E. Sivaniah, B. Ghalei, Enhanced PIM-1 membrane gas separation selectivity through efficient dispersion of functionalized POSS fillers, J. Membr. Sci. 539 (2017) 178–186, https://doi.org/10.1016/j.memsci.2017.05.072.

[175] W.F. Yong, K.H.A. Kwek, K.-S. Liao, T.-S. Chung, Suppression of aging and plasticization in highly permeable polymers, Polymers 77 (2015) 377–386, https://doi.org/10.1016/j.polymer.2015.09.075.

[176] W. Zhu, L. Wang, H. Cao, R. Guo, C. Wang, Introducing defect-engineering 2D layered MOF nanosheets into Pebax matrix for CO2/CH4 separation, J. Membr. Sci. 669 (2023) 121305, https://doi.org/10.1016/j.memsci.2022.121305.

[177] S. Wang, Y. Liu, S. Huang, H. Wu, Y. Li, Z. Tian, Z. Jiang, Pebax–PEG–MWCNT hybrid membranes with enhanced CO2 capture properties, J. Membr. Sci. 460 (2014) 62–70, https://doi.org/10.1016/j.memsci.2014.02.036.

[178] T. Zhou, L. Luo, S. Hu, S. Wang, R. Zhang, H. Wu, Z. Jiang, B. Wang, J. Yang, Janus composite nanoparticle-incorporated mixed matrix membranes for CO2 separation, J. Membr. Sci. 489 (2015) 1–10, https://doi.org/10.1016/j.memsci.2015.03.070.

[179] H. Wu, X. Li, Y. Li, S. Wang, R. Guo, Z. Jiang, C. Wu, Q. Xin, X. Lu, Facilitated transport mixed matrix membranes incorporated with amine functionalized MCM-41 for enhanced gas separation properties, J. Membr. Sci. 465 (2014) 78–90, https://doi.org/10.1016/j.memsci.2014.04.023.

[180] Q. Xin, H. Liu, Y. Zhang, H. Ye, S. Wang, L. Lin, X. Ding, B. Cheng, Y. Zhang, H. Wu, Z. Jiang, Widening CO2-facilitated transport passageways in SPEEK matrix using polymer brushes functionalized double-shelled organic submicrocapsules for efficient gas separation, J. Membr. Sci. 525 (2017) 330–341, https://doi.org/10.1016/j.memsci.2016.12.007.

[181] Q. Xin, H. Wu, Z. Jiang, Y. Li, S. Wang, Q. Li, X. Li, X. Lu, X. Cao, J. Yang, SPEEK/amine-functionalized TiO2 submicrospheres mixed matrix membranes for CO2 separation, J. Membr. Sci. 467 (2014) 23–35, https://doi.org/10.1016/j.memsci.2014.04.048.

[182] Q. Xin, Y. Gao, X. Wu, C. Li, T. Liu, Y. Shi, Y. Li, Z. Jiang, H. Wu, X. Cao, Incorporating one-dimensional aminated titania nanotubes into sulfonated poly (ether ether ketone) membrane to construct CO2-facilitated transport pathways for enhanced CO2 separation, J. Membr. Sci. 488 (2015) 13–29, https://doi.org/10.1016/j.memsci.2015.02.047.

[183] D. Peng, S. Wang, Z. Tian, X. Wu, Y. Wu, H. Wu, Q. Xin, J. Chen, X. Cao, Z. Jiang, Facilitated transport membranes by incorporating graphene nanosheets with high zinc ion loading for enhanced CO2 separation, J. Membr. Sci. 522 (2017) 351–362, https://doi.org/10.1016/j.memsci.2016.09.040.

[184] V. Martin-Gil, A. López, P. Hrabanek, R. Mallada, I.F.J. Vankelecom, V. Fila, Study of different titanosilicate (TS-1 and ETS-10) as fillers for mixed matrix membranes for CO2/CH4 gas separation applications, J. Membr. Sci. 523 (2017) 24–35, https://doi.org/10.1016/j.memsci.2016.09.041.

[185] Y. Li, X. Li, H. Wu, Q. Xin, S. Wang, Y. Liu, Z. Tian, T. Zhou, Z. Jiang, H. Tian, X. Cao, B. Wang, Anionic surfactant-doped Pebax membrane with optimal free volume characteristics for efficient CO2 separation, J. Membr. Sci. 493 (2015) 460–469, https://doi.org/10.1016/j.memsci.2015.06.046.

[186] W. Zhu, F. Liu, M. Gou, R. Guo, X. Li, Mixed matrix membrane containing metal oxide nanosheets for efficient CO2 separation, Green. Chem. Eng. 2 (2021) 132–143, https://doi.org/10.1016/j.gce.2020.11.009.

[187] S. Ding, X. Li, S. Ding, W. Zhang, R. Guo, J. Zhang, Ionic liquid-decorated nanocages for cooperative CO2 transport in mixed matrix membranes, Sep. Purif. Technol. 239 (2020) 116539, https://doi.org/10.1016/j.seppur.2020.116539.

[188] L. Yu, L. Hao, Y. Feng, J. Pang, M. Guo, L. Li, W. Fan, L. Fan, R. Wang, Z. Kang, D. Sun, Assembling ionic liquid into porous molecular filler of mixed matrix membrane to trigger high gas permeability, selectivity, and stability for CO2/CH4 separation, Nano Res. 17 (2024) 4535–4543, https://doi.org/10.1007/s12274-023-6329-z.

[189] B. Sasikumar, G. Arthanareeswaran, Interfacial design of polysulfone/Cu-BTC membrane using [Bmim][Tf2N] and [Dmim][Cl] RTILs for CO2 separation: Performance assessment for single and mixed gas separation, Sep. Purif. Technol. 295 (2022) 121315, https://doi.org/10.1016/j.seppur.2022.121315.

[190] S.N.A. Shafie, N.A.H. Md Nordin, S.M. Racha, M.R. Bilad, M.H.D. Othman, N. Misdan, J. Jaafar, Z.A. Putra, M.D.H. Wirzal, Emerging ionic liquid engineered polymeric membrane for carbon dioxide removal: a review, J. Mol. Liq. 358 (2022) 119192, https://doi.org/10.1016/j.molliq.2022.119192.

[191] I. Angelidaki, L. Treu, P. Tsapekos, G. Luo, S. Campanaro, H. Wenzel, P. G. Kougias, Biogas upgrading and utilization: current status and perspectives, Biotechnol. Adv. 36 (2018) 452–466, https://doi.org/10.1016/j.biotechadv.2018.01.011.

[192] A. Toledo-Cervantes, J.M. Estrada, R. Lebrero, R. Muñoz, A comparative analysis of biogas upgrading technologies: photosynthetic vs physical/chemical processes, Algal Res. 25 (2017) 237–243, https://doi.org/10.1016/j.algal.2017.05.006.

[193] R. Rodero, R. Lebrero, E. Serrano, E. Lara, Z. Arbib, Technology validation of photosynthetic biogas upgrading in a semi- industrial scale algal-bacterial photobioreactor, Bioresour. Technol. 279 (2019) 43–49, https://doi.org/10.1016/j.biortech.2019.01.110.

[194] A. Francisco López, T. Lago Rodríguez, S. Faraji Abdolmaleki, M. Galera Martínez, P.M. Bello Bugallo, From biogas to biomethane: an in-depth review of upgrading technologies that enhance sustainability and reduce greenhouse gas emissions, Appl. Sci. 14 (2024), https://doi.org/10.3390/app14062342.

[195] E. Esposito, L. Dellamuzia, U. Moretti, A. Fuoco, L. Giorno, J.C. Jansen, Simultaneous production of biomethane and food grade CO2 from biogas: an industrial case study, Energy Environ. Sci. 12 (2019) 281–289, https://doi.org/10.1039/C8EE02897D.

[196] F. Ardolino, G.F. Cardamone, F. Parrillo, U. Arena, Biogas-to-biomethane upgrading: a comparative review and assessment in a life cycle perspective, Renew. Sustain. Energy Rev. 139 (2021) 110588, https://doi.org/10.1016/j.rser.2020.110588.

[197] G.O. Yahaya, I. Mokhtari, A.A. Alghannam, S.-H. Choi, H. Maab, A.A. Bahamdan, Cardo-type random co-polyimide membranes for high pressure pure and mixed sour gas feed separations, J. Membr. Sci. 550 (2018) 526–535, https://doi.org/10.1016/j.memsci.2017.10.063.

[198] D.J. Harrigan, J. Yang, B.J. Sundell, J.A. Lawrence, J.T. O'Brien, M.L. Ostraat, Sour gas transport in poly(ether-b-amide) membranes for natural gas separations, J. Memb. Sci. 595 (2020) 117497, https://doi.org/10.1016/j.memsci.2019.117497.

[199] D.J. Harrigan, J.A. Lawrence, H.W. Reid, J.B. Rivers, J.T. O'Brien, S.A. Sharber, B. J. Sundell, Tunable sour gas separations: simultaneous H2S and CO2 removal from natural gas via crosslinked telechelic poly(ethylene glycol) membranes, J. Memb. Sci. 602 (2020) 117947, https://doi.org/10.1016/j.memsci.2020.117947.

[200] J.A. Lawrence, D.J. Harrigan, C.R. Maroon, S.A. Sharber, B.K. Long, B.J. Sundell, Promoting acid gas separations via strategic alkoxysilyl substitution of vinyl-added poly(norbornene)s, J. Memb. Sci. 616 (2020) 118569, https://doi.org/10.1016/j.memsci.2020.118569.

[201] H. Jasuja, G.W. Peterson, J.B. Decoste, M.A. Browe, K.S. Walton, Evaluation of MOFs for air purification and air quality control applications: ammonia removal from air, Chem. Eng. Sci. 124 (2015) 118–124, https://doi.org/10.1016/j.ces.2014.08.050.

[202] N. Gargiulo, A. Peluso, P. Aprea, O. Marino, R. Cioffi, E. Jannelli, S. Cimino, L. Lisi, D. Caputo, Chromium-based MIL-101 metal organic framework as a fully regenerable D4 adsorbent for biogas purification, Renew. Energy 138 (2019) 230–235, https://doi.org/10.1016/j.renene.2019.01.096.

[203] E. Gulcay-Ozcan, P. Iacomi, Y. Ko, J.-S. Chang, G. Rioland, S. Devautour-Vinot, G. Maurin, Breaking the upper bound of siloxane uptake: metal–organic frameworks as an adsorbent platform, J. Mater. Chem. A 9 (2021) 12711–12720, https://doi.org/10.1039/D1TA02275J.